Brandenburgische
Technische Universität
Cottbus - Senftenberg

Faculty of Environment and Natural Science

Institute of Biotechnology

Master Thesis

The specific Cell Entry Pathway of the Human Endogenous Retrovirus-K (HML-2) and the Role of Heparan Sulfate Proteoglycans

presented by

Philipp Geppert

Produced in department 18 „HIV and other Retroviruses“

at the Robert Koch Institute

to obtain the academic degree „Master of Science“ (M.Sc.)

under supervision of Prof. Dr. N. Bannert

Berlin, December 2018

ROBERT KOCH INSTITUT

1st supervisor: **Dr. rer. nat. Barbara Hansen**

BTU Cottbus – Senftenberg

Faculty of Environment and Natural Science, Institute of Biotechnology

2nd supervisor: **Prof. Dr. Norbert Bannert**

Robert Koch Institute

Department 18 „HIV and other Retroviruses“

Dedicated to my family, girlfriend and daughter

Table of contents

Abstract

A lot of viruses have been shown to use a wide variety of attachment molecules on cell surfaces and exploit them as receptors and establish an infection (Rostand and Esko, 1997). Viral entry, spread and pathogenesis can be better understood by identification of the cell surface receptor(s) of particular virus targets (Shukla and Spear, 2001). Virus entry is a two-step process, with the first step being attachment of the virus to a primary receptor, followed by the interaction with a co-receptor that is usually a cell-specific transmembrane protein (Shukla *et al.*, 1999; Summerford and Samulski, 1998). Understanding the interaction between proteins on the surface of virus particles and the cell surface receptors which are used by the virus particles to enter cells is essential to understand viral tropism, which further helps in creating effective antiviral therapies.

Several published studies have suggested that a number of viruses use the heparan sulfate (HS) component of cell surface heparan sulfate proteoglycans (HSPGs), as an main receptor to attach to cells (Liu and Thorp, 2002; Rostand and Esko, 1997; Zhu *et al.*, 2011). HS is a glycosaminoglycan (GAG) composed of repeating disaccharides of glucosamine and hexuronic acid, joined in alternating sequences by 1,4-glycosidic linkages, which gives these carbohydrate chains the flexibility to bind to many different proteins (Li and Vlodavsky, 2009; Lindahl, 1990). There are a lot of HS-binding viruses from different families and include herpes simplex virus (HSV) (WuDunn and Spear, 1989), human papillomavirus (HPV) (Giroglou *et al.*, 2001), hepatitis B virus (HBV) (Cooper *et al.*, 2005), respiratory syncytial virus (RSV) (Hallak *et al.*, 2000), foot-and-mouth disease virus (FMDV) (Jackson et al., 1996) and the human immunodeficiency virus type 1 (HIV-1) (Roderiquez *et al.*, 1995).

For this reason, it was important to analyze which proteins are responsible for the entry of HERV-K (HML-2). Therefore, the receptors ASCT1/2 (for syncytin-1) and MFSD2A (for syncytin-2) were transfected into HEK293T cells. Infection with various pseudotyped HIV showed that viral entry into the cells could not be increased. For this reason, it could be assumed that syncytin receptors are not primarily responsible for entry. This was the reason that new receptor candidates had to be used for further experiments. Previos work by N. Bnnert and A. Richter compared different gene profiles of successfully infected cells with HERV-K and thus identified potential receptors that might be specifically involved in the onset of the virus. These receptors were the G protein-coupled receptor 56 and 161, the cell surface receptor CD63, the neural cell adhesion molecule L1CAM, the golgi sorting receptor sotilin-1 and the cell surface protein neuroligin-1. Overexpression of these receptors revealed that the g protein-coupled receptor 56 must have a crucial role in the onset of HERV-K (HML-2), as it could increase the infection rate by 3-fold.

Furthermore, this study investigated the influence of heparan sulfates on the entry of HERV-K into the cells. For this, free heparan sulfate was incubated before infection with the cells and pseudotyped HIV. It turned out that an increase of the heparan sulfate concentration up to 400µg/ml led to a reduction of the infection rate up to 40%. A change in the cell surface profile was achieved by enzymatic digestion with heparinase I and III and a chemical reaction with sodium chlorate. While heparinase is responsible for the digestion of heparan sulfates, sodium chlorate prevents the sulfation of glycosaminoglycan's. Both experiments showed that with increasing concentration, the infection rate of HERV-K decreased. The viral entry after enzymatic digestion was reduced up to 50% and after chemical inactivation of sulfation by up to 30%. Another approach to verify HS functionality was the overexpression of a specific heparan sulfate. Syndecan-1 is a transmembrane (type I) heparan sulfate proteoglycan and is a member of the syndecan family. This protein was amplified in HEK293T and HCT116 cells and infected with pseudotyped HIV. However, analysis of the resulting luciferase revealed that this had no effect on the rate of infection. In further experiments, syndecan-1 was reduced by means of special shRNAs on the cell surface. A short hairpin RNA is an artificial RNA molecule with a tight hairpin turn. The expression of shRNA in the cell lines was done by the transfection of specific plasmids and blocks the specific mRNA of the examined gen. The reduction of the syndecan-1 level on the cell surface led to a reduction in the infection rate of HERV-K down to 30% in HEK293T cells. The entry of the viruses into the cells should be measured by means of the formed firefly luciferase. In the luciferase assay, reporter constructs carrying a firefly luciferase gene behind a CMV promotor and after this, the sequence which is important to produce virus particles.

Based on these facts, it can be said that various heparan sulfates and GPR56 might play a crucial role in the entry of HERV-K (HML-2). This should be one of the main theses for future work on this topic.

Abbreviations

AIDS	Acquired Immune Deficiency Syndrome
ALV	Avian Leukemia Virus
CD	Cluster of differentiation
CVA16	Coxsackievirus A16
DNA	Deoxyribonucleic acid
Env	Envelope
ERV	Endogenous Retrovirus
FACS	Fluorescence-activated cell sorting
FV	Foamy Virus
Gag	Group-specific antigen
GFP	Green fluorescent protein
HCV	Hepatitis C Virus
HERV	Human Endogenous Retrovirus
HIV	Human Immunodeficiency Virus
HML	Human MMTV-like
HS	Heparansulfat
HSPG	Heparan sulfate proteoglycan
HTLV	Human T-cell Leukemia Virus
LTR	Long terminal repeats
MLV	Murine Leukemia Virus
MMTV	Mouse Mammary Tumor Virus
Nef	Negative factor
PAPS	3’-Phosphoadenosin-5’-phosphosulfat
PERV	Porcine Endogenous Retrovirus
PIC	Preintegration complex
Pol	Polymerase
Pro	Viral protease
RNA	Ribonucleic acid
RSV	Rous Sarcoma Virus
RT	Reverse Transcriptase
SDC1	Syndecan-1
tPBS	tRNA primer binding site
Vpr	Viral protein rapid
Vpu	Viral protein out

Index of figures

Index of tables

1. Introduction

1.1 Retroviruses

Retroviruses compromise enveloped viruses carrying two homologous RNA single plus strands in the virus core. These are not translated directly as other RNA viruses, but rewritten with the help of viral reverse transcriptase (RT) into double-stranded DNA and incorporated into the host genome. They mainly infect animal and human cells from mammals, birds, reptiles, amphibians to fish. Retroviruses are found in all vertebrates and usually have very high host specificity.

At the beginning of the 19th century, retrovirus-induced disease such as bovine leukemia or pulmonary adenomatosis in sheep were known but not their cause (Weiss, 2006). In 1908, Ellermann and Bang examined the first oncogenic retrovirus, the avian leukemia virus (ALV) and showed that cell-free filtrate can be used to transfer chicken leukemia to other chickens (Ellerman V. and Bang O., 1908). Three years later, Rous transferred the Rous sarcoma virus (RSV) to healthy chickens with extracts from chicken sarcoma. These then also developed tumors (Rous P., 1911). 54 years later he received the Nobel Prize for it. In 1936, another tumor-inducing retrovirus was discovered, the mouse mammary tumor virus (MMTV), which has tumors in the mammary gland of mice is related (Bittner JJ., 1936). A key step in the history of retroviruses has been the discovery of RNA in RSV particles (Crawford LV. and Cawford EM., 1961). In 1964, Howard M. Temin presented his provirus hypothesis using the example of RSV, which states that RNA integrates tumor viruses into the host genome (Temin HM, 1964; Temin HM, 1963). By the discovery of reverse transcriptase by David Baltimore and Howard M. Termin, the RNA tumor viruses were ultimately renamed retroviruses in 1974 (Baltimore D., 1975). This discovery rejected an accepted dogma of molecular biology. It said that the flow of information in cells always goes from DNA to protein via RNA (Coffin JM. *et al.*, 1997).

In the early 1970s, the first viral proteins were described and in 1978 the long terminal repeats (LTRs) were identified (Ju G. and Skalka AM., 1980). The description of the first human T-cell leukemia virus type-1 (HTLV-1), was made two years later by Robert C. Gallo (Gallo RC., 2005; Poiesz BJ. *et al.*, 1980). In 1983, Luc Montagier and Francoise Barré Sinoussi discovered the most prominent human phagocytic retroviruses, human immunodeficiency virus type 1 (HIV-1), followed by HIV-2 in 1983 (Barré-Sinoussi F. *et al.*, 1983; Clavel F. *et al.*, 1986). HIV-1 induces AIDS (Acquired Immune Deficiency Syndrome) and has led to a strong drive for retro virology research in recent decades. In 2008, an estimated 33.4 million people worldwide were infected with HIV. Every year about two million people die as a result of the infection and about the same number of new infections with HIV occurs in the same period. The pathogenic agent HTLV-1 applies as cause of adult T-cell leukemia (ATL), but also of HTLV-1-associated myelopathy (Alves and Dourado, 2010). HTLV-2, on the other hand, leads to T-cell lymphoma, hairy cell

leukemia and neurological diseases. However, it should be distinguished that HTLV-1 infected CD4+ and HTLV-2 CD8+ lymphocytes (Cereseto *et al.*, 1996; Poiesz BJ. *et al.*, 1980).

Retroviruses are divided into simple and complex retroviruses. Complex retroviruses are distinguished by regulatory genes in the viral genome, which lead to the expression of accessory proteins. The current phylogenetic taxonomy of Retroviridae has been established by the International Committee on Taxonomy of Viruses (ICTV) consisting of 500 international virologists. A distinction is made between the subfamilies Orthoretrovirus (Orthoretrovirinae) and Spumaretrovirus (Spumaretrovirinae). Orthotrophic viruses are divided into six genera. These included on the one hand the alpha, gamma and epsilon retroviruses with a simple genome and on the other hand the beta and delta retroviruses, as well as the lentiviruses with a complex genome (Weiss, 2006).

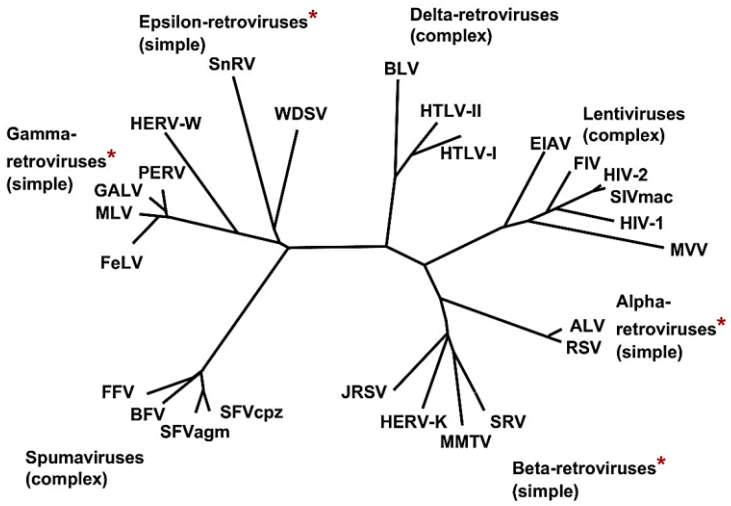

Figure 1: Phylogenetic pedigree of retroviruses
The seven genera of the Retroviridae and their representatives. The red star means that there are exogenous as well as endogenous representatives (Modified from: (Weiss, 2006).

Before comparisons of phylogenetic relationships were made, retroviruses were distinguished by their morphological features in electron microscopy and classified taxonomically. Here one distinguished between A-, B-, C- and D-type retroviruses depending on their assembly form and the extracellular, morphological features of their viral particles (Coffin JM. *et al.*, 1997; Nermut and Hockley, 1996).

1.1.1 Endogenous Retroviruses (ERV)

Endogenous retroviruses (ERVs) are exogenous retroviruses that infect vertebrate germ cells, are integrated into the host genome as provirus and transmitted to the offspring via the germ line according to the Mendel´s laws. This path of inheritance is called vertical inheritance. Thus, all somatic cells that emerge from infected germ cells carry the provirus (Weiss, 2006). There are dozens to thousands of ERVs in the vertebrate genome (Herniou *et al.*, 1998). Over millions of years, these have been subjected to mutations, deletions and transpositions that have led to inactive proviruses over time. Nevertheless, replication-competent proviruses are capable of releasing functional viral particles, such as mouse mammary tumor viruses (Fiebig *et al.*, 2006; Weiss, 2006). Some animal retroviruses thus form both exogenous and endogenous forms. In addition to MMTV and MLV in mice, these include ALV in chickens, the Jaagsiekte sheep retroviruses in sheep, porcine endogenous retroviruses (PERV) in swine and feline leukemia virus in cats (Coffin JM. *et al.*, 1997). The viral particles emerging from the endogenous form again infect somatic cells via the exogenous pathway or reinfect already infected cells (van Nie *et al.*, 1977; Weiss, 2006). This form of inheritance is called horizontal inheritance (Figure 2a).

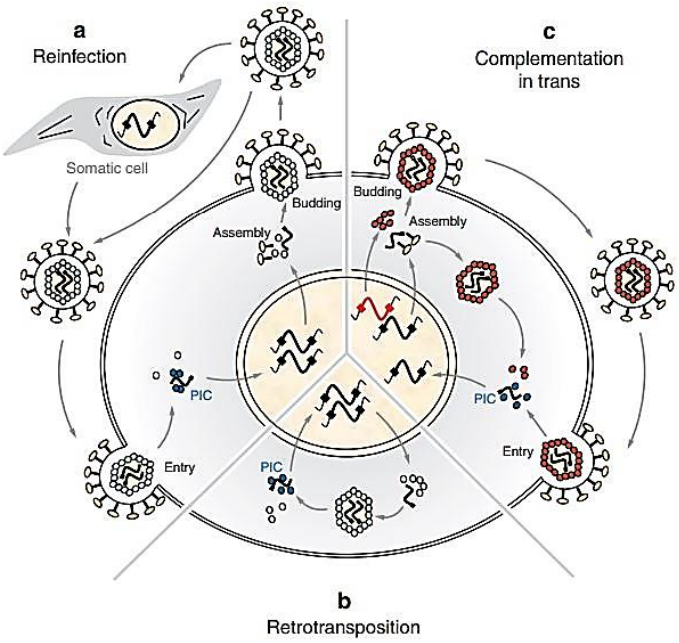

Figure 2: Proliferation of endogenous retroviruses
Endogenous retroviruses have three possibilities of propagation. a) In reinfection the provirus is able to form functional viral particles, the other somatic cells or the host cell again can infect (horizontal path). b) Retransposition is the intracellular multiplication, which also leads to the integration of new proviruses into the cell genome. c) The complementation in trans describes the recombination of viruses. If the provirus is partially defective, these can be replaced by components of other retroviruses that have infected the cell (red). PIC: preintegration complex (Modified from: (Bannert and Kurth, 2006).

Some endogenous retroviruses multiply intracellularly only. This process, known as retrotransposition, does not require a functional env gene and re-integrates the provirus into the host genome (Figure 2b).

A third propagation process, which is based on recombination, is called complementation in trans and occurs in proviruses with partially inactive genes. These are replaced by the expression of active genes from other proviruses, which can lead to the formation of functional particles (Figure 2c, (Bannert and Kurth, 2006). In late 1960s, the first ERVs were discovered. These were the cancer-causing viruses MLV, MMTV and ALV (Weiss, 2006). Today, it is known that the retroviral part in the genome of vertebrates accounts for about five to ten percent (Herniou *et al.*, 1998; Smit, 1999). More than 3300 endogenous retroviruses are already known for humans and chickens. Comparison of viral highly conserved pol sequences (800 to 1100 amino acids) demonstrated a wide distribution of ERVs. In 2007, the first endogenous lentivirus in European rabbits was found, which is more than seven million years old and has complete lentiviral gag, pol and env domains (Katzourakis *et al.*, 2007).

1.1.2 Human Endogenous Retroviruses (HERV)

The human genome consists of 8% retroviral elements with terminal LTRs, 4.7% of which are human endogenous retroviruses (HERVs) (Bannert and Kurth, 2004; Beimforde *et al.*, 2008; Lander *et al.*, 2001). HERVs were also once exogenous retroviruses that infected human endocrine cells, endogenized and multiply integrated into the genome by reinfection and retrotransposition (Gifford and Tristem, 2003). The human genome project of 2001 identified several thousands HERVs in the human genome based on sequence comparisons with known mammalian retroviruses (Gifford RJ, 2006; Lander *et al.*, 2001). Human endogenous retroviruses are classified into three classes because of their similarities with beta, gamma or spumaviruses. The subdivision into HERV subclasses usually follows the primer binding site, which defines the specific tRNA that acts as a primer for the reverse transcriptase. In the case of HERV-K, the lysine tRNA serves as a primer (Andersson *et al.*, 1999; Bock and Stoye, 2000). The best preserved elements belong to the HERV-K (HML-II) family and are classified as betaretroviruses based on their relationship to the exogenous mouse mammary tumor viruses (MMTV). HML stands for 'human MMTV-like' (Hohn *et al.*, 2013; Hohn *et al.*, 2016).

HERVs play an important physiological and pathological role. In 1992 the physiological influence of the 5'LTR of HERV-E on the expression of its from C-terminal α-amylase gene could be detected. The promotor function of the LTR thereby enhances the production of the sugar-splitting enzymes of the salivary gland and thus leads to a faster utilization of carbohydrates in the diet (Ting *et al.*, 1992). Another example is the env genes of HERV-W and HERV-FRD, better known as syncytin-1 and syncytin-2, which influence placental development (Bannert *et al.*, 2018). Syncytin-1 is involved in the fusion of the cytotrophoplasts cells and thus leads to the formation of the polynuclear syncytiotrophoblast (Blond *et al.*, 1999; Blond *et al.*, 2000; Mi *et al.*, 2000; Pötgens *et al.*, 2004). Syncytin-2 carries through its immunosuppressive properties of mother-to-child tolerance during pregnancy (Malassiné *et al.*, 2007). Recent studies have pointed to the expression of the HERV-K envelope protein in cells of the placental

cytotrophoblast, but not in the sncytiotrophoblast. One also suspects immunosuppressive properties and thus a protective function against fetal rejection by the maternal immune system (Kämmerer *et al.*, 2011). However, HERV-K has also been pathologically linked to germ cell tumors and melanomas (Büscher *et al.*, 2005; Götzinger *et al.,* 1996; Krone and Grange, 2010). But other HERVs also play an important role in disease education. In prostate cancer an increased expression of the envelope protein of HERV-E was found, but not in healthy tissue (Wang-Johanning *et al.*, 2003). HERV-W is associated with multiple sclerosis and psychiatric disorders such as schizophrenia (Antony *et al.,* 2011; Leboyer *et al.*, 2013). In addition, multiple sclerosis HERVs have been implicated in other autoimmune diseases, such as type 1 diabetes mellitus, rheumatoid arthritis and lupus erythematosus (Balada *et al.*, 2010).

1.2 Structure and replication of retroviruses

1.2.1 Morphology of retroviral particles

Retroviruses are enveloped viruses with a diameter of 80-120nm and possess aikosahedral, cylindrical or conical core. They consist of 65% proteins, 30% lipids, 3% carbohydrates and 2-3% RNA (Coffin JM. *et al.*, 1997; Vogt VM, Simon MN, 1999). Basically, a morphologically distinction is made between immature and mature, extracellular retroviral particles. Immature particles are released by cells and mature by processing of the polystructure protein gag by viral protease. Both forms have a viral envelope membrane enriched with sphingolipids, cholesterol and other components of lipid rafts (Aloia *et al.*, 1993; Quigley *et al.*, 1971).

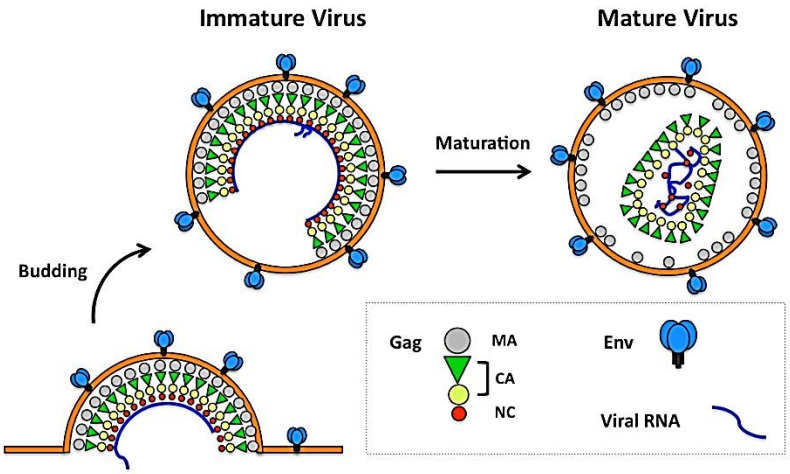

Figure 3: Gag and Retrovirus assembly
The cartoon shows three stages in retrovirus morphogenesis: a partially assembled particle on the host cell plasma membrane, an immature particle that is composed of a paracrystalline gag structure and a mature virus particle that has a distinct core. Gag is a polyprotein including matrix (MA), capsid (CA) and nucleocapsid protein (NC) domains. Env represents the trimeric envelope protein matrix. The figure is adapted from two review papers (Ganser-Pornillos *et al.*, 2008; Maldonado *et al.*, 2014).

Their surface is also homogeneously associated with viral, glycosylated envelope protein which spans the viral transmembrane protein consisting of about 20 hydrophobic amino acids (Özel *et al.*, 1988). Below the viral membrane of immature particles is a homogeneous layer which is formed by the precursor protein gag. It accounts for about three quarters of the protein content of viral particles and shows itself in transmission electron microscopy as an electron-dense layer under the envelope membrane (Coffin JM. *et al.*, 1997). If the precursor protein gag is split into its individual structural proteins as part of the maturation by the viral protease, mature particles are formed. In contrast to the immature particles, these are characterized by an electron-dense core. After maturation, the matrix protein remains close to the membrane. The capsid proteins form into the virus core, the capsid. It has the ribonucleoprotein complex, consisting of two homologous RNA single plus strands and nucleocapsid proteins that bind and condense the RNA (Nermut and Hockley, 1996). In addition, the capsid contains other viral proteins, such as the reverse transcriptase, the integrase and the viral protease.

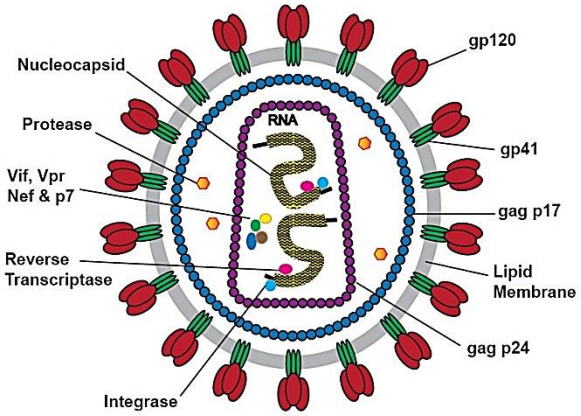

Figure 4: Schematic construction of an HIV particle
Lipid membrane with heterodimeric complex of membrane glycoproteins gp41 and gp120; Matrix consisting of matrix proteins p17; Capsid consisting of capsid proteins p24; Ribonucleoprotein complex consisting of nucleocapsid protein p7, reverse transcriptase, viral RNA genome and integrase; accessory proteins viral infectivity factor (Vif), viral protein rapid (Vpr), viral protein out (Vpu) and negative factor (Nef) (source: eenzyme).

1.2.2 Viral genome and provirus

Retroviruses have a 7 to 12 kilo base (kb) genome consisting of two homologous RNA single strands in the plus strand orientation. The genome of the retroviruses basically consists of the four genes gag, pro, pol and env. All genes having an open reading frame (ORF). The genes gag and env are structural genes. The gag gene creates the group specific antigen. It is a polystructure protein and includes the major structural proteins of all retroviruses: matrix, capsid and nucleocapsid protein (figure 3). In addition, most gag proteins have other proteins of different functions (Coffin JM. *et al.*, 1997). They are located either at the C-terminus of gag or between the previously mentioned structural proteins. Some of these

proteins have one or more L-domains and are therefore crucial for the budding and release of viral particles. The pro gene encodes the viral protease, pol the viral enzymes reverse transcriptase, integrase and RNaseH and env the envelope protein. Env is also a precursor protein consisting of signal peptide, surface glycoprotein and transmembrane protein. In contrast to the gag protein, it is processed before incorporation into viral particles (Coffin JM. *et al*., 1997; Kurth R. and Bannert N., 2010). Complex retroviruses also have regulatory genes. They lead to the expression of accessory proteins, which can influence host factors and decisively influence the replication cycle (Coiras *et al.*, 2010).

When the viral genome is integrated into the DNA of the host, it is called a provirus. The viral genes are flanked by an LTR, which are always in the same orientation (Reuss and Schaller, 1991). LTRs are 200 to 600 base pairs long, regulatory DNA sequences that are essential for the integration or reintegration of retro elements into the host genome. In addition, they serve as a binding site for the transcription factors and contain all signal sequences for the initiation, amplification and control of gene expression. An LTR is composed of U3 region, which includes promotor and enhancer, R region and U5 region. The viral RNA is flanked at the 5' end by a 5' cap structure followed by R and U5 regions. Behind the U5 region is directly the primer binding site (tPBS) for the cell own transfer RNA. This initiates reverse transcription since the tRNA acts as a primer in this case. The tPBS follows the Ψ site, the packaging signal of the retroviral RNA. At the 3' end of the viral RNA is the R and U3 regions with a 3' polyadenylation, also termed as poly-A-tail.

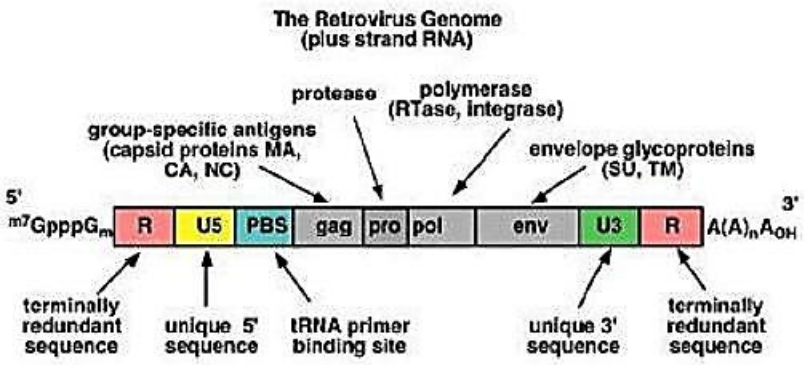

Figure 5: General structure of a retroviral genome
The long terminal repeats (LTRs) have sequences needed for the regulation and initiation of transcription within the unique sequences 3 and 5 regions (Anakok OF, 2016).

1.2.3 Replication cycle

The replication of retroviruses begins by infection of the host cell. The virus, mediated by its glycosylated cot proteins, attaches to specific receptors of the cell. It leads to the fusion of the virus envelope with the plasma membrane or to the endocytosis of the entire viral particle. Upon entry into the cell, the envelope-less capsid undergoes a conformational change, releases some of its subunits and becomes permeable to nucleotides (Modrow S. *et al.*, 2009). This reverse transcriptional complex includes the ribonucleotide complex associated with the reverse transcriptase. The binding of the specific tRNA to the primer binding site of the viral RNA initiates the process of reverse transcription. The viral genetic information is transcribed into double-stranded, proviral DNA. The viral RNA is subsequently hydrolytically degraded by the viral RNaseH. The resulting pre-integration complex of proviral DNA and proteins is transported in the lentiviruses from the cytoplasm through the nuclear pores into the cell nucleus. These include nuclear import factors as well as accessory viral proteins, such as Vpr in HIV-1 (Bukrinsky *et al.*, 1993; Freed, 2001). Pre-integration complexes of other retroviruses are only able to migrate into the cell nucleus during mitosis, since nuclear-transport-promoting factors are lacking. In the nucleus, the proviral DNA then integrates into the euchromatic host genome via integrase. This can lead to the destruction, inactivation or activation of cell genes. The integration of the provirus is essential for the expression of viral proteins and is inherited by cell division (Weiss, 2006). When transcription of viral genes occurs, depending on the activity state of the host cell, various viral mRNA species are observed (Reed, 2003).

On the one hand, this is the full-length mRNA, which is also available as a viral genome due to the packaging signal. Their translation leads to the synthesis of the precursor proteins gag, gag-pro and gag-pro-pol (Bannert and Kurth, 2004; Swanstrom and Wills, 1997). On the other hand, it's possible to find single and multiple spliced mRNA. Splicing is an essential process to produce multiple proteins encoded in a transcript independently expressing each other (Bodem *et al.*, 2011). In addition, due to cellular control mechanisms, only spliced mRNA can be exported from the cell nucleus. To get around this, complex retroviruses have specific shuttle proteins that allow the transport of viral full-length mRNA into the cytoplasm (Cullen, 2002; Hanke *et al.*, 2013; Wodrich and Kräusslich, 2001). The expression of almost all viral proteins takes place on free, in the cytoplasmic ribosomes or ribosome chains (polysomes) instead (Tritel and Resh, 2000). The transport of the viral proteins is then carried out directly or via endosomal transport pathway to the plasma membrane. The precursor protein env, on the other hand, is formed on the rough endoplasmic reticulum (rER) by translation of single spliced mRNA and integrated directly into the ER membrane (Checkley *et al.*, 2011; Teissier *et al.*, 2010). This is followed by vesicular transport via the trans-Golgi network to the plasma membrane. Depending on the site of assembly, the viral particles are then released via exocytosis or budding from the plasma

membrane and mature extracellularly by processing the gag precursor proteins by means of viral protease (George *et al.*, 2011; Kraus *et al.*, 2011; Ono, 2009).

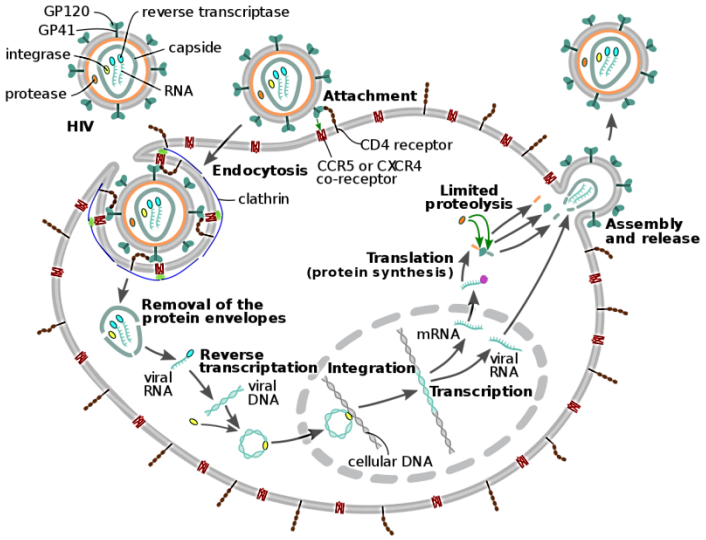

Figure 6: HIV replication cycle
The replication cycle of retroviruses begins with the receptor-dependent binding of the virus to the host cell. Depending on the virus, the capsid is internalized by the fusion of the viral envelope with the cell membrane or endocytosis. The transcription of single-stranded RNA into double-stranded DNA is carried out by means of reverse transcriptase in the complex. The resulting pre-interglacial complex is imported into the nucleus and the viral genome is integrated into the host DNA as a provirus. The mRNA resulting from the transcription of the viral DNA is partially differentially spliced before nuclear export and serves for protein expression. Full-length mRNA and viral proteins assemble on cellular membranes into viral particles. These are released and mature extracellularly (Jmarchn, 2017).

1.2.4 Entry of HIV in the target cell

The entry of HIV into the host cell is mediated by the interaction of the virus with the CD4 receptor and another chemokine receptor. The CD4 receptor is a T-cell receptor which is used to display antigens on the T-cell and interacts with the major histocompatibility complex II (MHC II) of the immune system. The virus binds with the immunodominant V3 loop of the external glycoprotein gp120 to the monomeric glycoprotein receptor CD4. This is present on the cell surface of T-lymphocytes, Monocytes and macrophages (Bowers *et al.*, 1997). After the interaction between gp120, CD4 and subsequently also the appropriate co-receptor, the resulting cascade of conformational changes causes membrane fusion through the transmembrane glycoprotein gp41 is initiated. The chemokine receptors are subdivided according to the amino acid motifs of their natural ligands into the following groups: CXC, CC, CX3C or C. HIV can interact with different co-receptors, because of its variability. Currently, HIV is differentiated into two major variants after use of the co-receptor. The T-cell tropics HIV isolate (X4 virus) use the chemokine receptor CXCR4, while the macrophage-tropic isolate (R5 virus) use the receptor CCR5 (Deng *et al.*, 1996; Feng *et al.*, 1996). However, HIV can also use other so-called alternative co-receptors (orphan receptors) (Alkhatib and Berger, 2007).

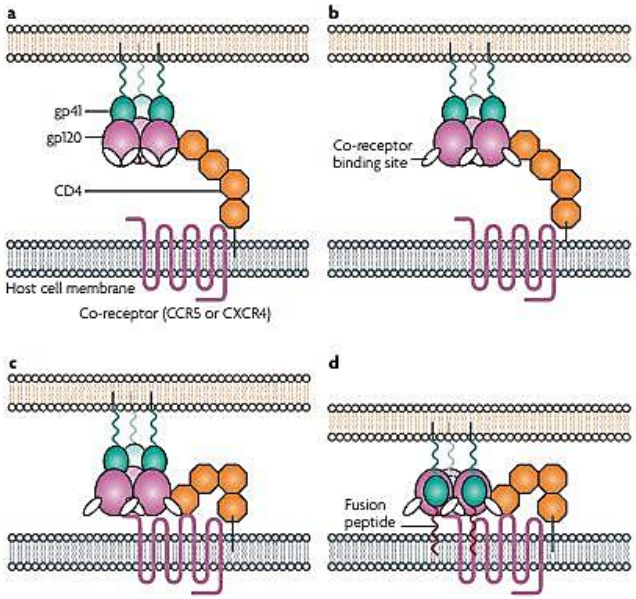

Figure 7: Human immunodeficiency virus (HIV) co-receptors.

When the HIV glycoprotein gp120 binds to CD4 (a), it induces a conformational change in gp120 that exposes the co-receptor binding site (b); this is a complex domain comprising the V3 loop and specific amino-acid residues in CD4, collectively termed the "bridging sheet". Exposure of the co-receptor binding site permits binding of gp120 to the co-receptor (c). Co-receptor binding induces conformational change in gp41 and insertion of the fusion peptide into the host cell membrane (Clercq, 2007).

1.3 Heparan sulfate proteoglycans

HSPG´s are a group of proteins which belongs to the group of glycosaminoglycan's and have at least one covalently linked heparan sulfate (HS) side chain. The basic structure of the unbranched HS side chains is an alternating sequence of glucuronic acid and N-acetylglucosamine, which are linked to beta-1,4- and alpha-1,4-glycosidically. The polymer is modified at various points by sulfation and epimerization. Because of the variability of these modifications, there are approximately thirty different disaccharides, and thus probably the formation of the most complex polysaccharides in mammalian cells (Esko, 1991; Kjellén and Lindahl, 1991). The modifications result in greater conformational flexibility and a strong negative charge, thereby supporting the electrostatic binding interactions of the proteoglycans. Some of these interactions are very specific and are mediated by defined sugar sequences within HS side chains (Turnbull *et al.*, 1992).

The primary structure of various heparan sulfate proteoglycans was determined by cloning of cDNAs. As a result, two forms of membrane associations could be detected. On the one hand anchoring via a transmembrane domain (syndecan family), on the other hand binding via GPI to the plasma membrane (glypikan family) (David *et al.*, 1990).

The family of syndecans consists of syndecan-1, syndecan-2 or fibroglycan, syndecan-1 or N-syndecan and syndecan-4, also called amphiglycan (David *et al.*, 1990). All syndecans have an extracellular domain whose sequence similarity of 10 to 20%. The transmembrane domain and the short cytoplasmic domain of these four proteins, on the other hand, have 60-70% sequence similarity. The transmembrane domain is responsible, among other things, for the formation of cell surface complexes (Asundi and Carey, 1997). Syndecan-1 is the predominant proteoglycan in epithelial cells. In fibroblasts, on the other hand, it is of little importance and it is still expressed at certain times during embryonic development (Kim *et al.*, 1994). In addition to heparan sulfates syndecan-1 also has chondroitin sulfates. Syndecan-2 is found mainly on fibroblasts and endothelial cells, while it lacks in most epithelial cells. In contrast, syndecan-4 is a ubiquitous proteoglycan (David *et al.,* 1990).

HS side chains bind a variety of growth factors, extracellular matrix factors and other proteins, indicating that HS side chains bind to cell adhesion or regulation of cell division activity (Carey, 1997). In addition, it is known that various pathogens interact with the HS side chains. This includes the binding of the human cytomegalovirus (Compton *et al.*, 1993) and herpes simplex virus (Shieh, 1992), the binding of the bacteria Borrelia burgdorferi (Isaacs, 1994), Chlamydia trachomatis (Chen *et al.,* 1996), Staphylococcus aureus (Liang *et al.*, 1995) and the protozoa Leishmania (Love *et al.*, 1993) and Trypanosoma cruzi (Ortega-Barria and Pereira, 1991).

1.4 Aim of the work

The human genome consists of about 8% endogenous retroviruses, some of them are highly conserved to generate functional proteins and viral particles. Probably the best preserved proviruses belong to the family HERV-K (HML-2). For viral infection, the expression of functional HERV-K (HML-2) envelope proteins is of crucial importance. These not only mediate the first cell contact, initiate the fusion of virus and host membrane, but also determine the host specificity for the infection of a particular tissue, cell type or organism. Endogenously expressed HERV-K (HML-2) envelope proteins are also able to be incorporated into foreign retroviruses and thus alter their cell tropism.

Because of the specificity of viral coat proteins, it is important to understand which structures and receptors facilitate the virus entry into the host cell. For this reason, the aim of the work is to examine different receptors on the host cell and to determine which of these proteins are responsible for the entry of HERV-K (HML-2). In order to investigate differences in the entry of viral particles, various membrane-bound receptors are to be overexpressed in a selected cell line. This overexpression should lead to a facilitated entry into the host cell. The plasmids which can be used for the receptors are

brought into the cells by PEI transfection, because a high transfection efficiency is to be expected. Due to the different protein tags of the receptors, they can be analyzed by western blots or EGFP fluorescence. Since the modified viruses have the ability to form luciferase within the cell, a luciferase assay is used to determine the amount of viral infection.

Due to the broad tropism of HERV-K, it can be concluded that ubiquitous membrane-bound macromolecules, rather than tissue-specific proteins, are candidates for cellular receptors that mediate viral binding or entry into the cell. Therefore, another goal of this work is to study the function of one of the important glycosaminoglycan's. Heparan sulfate is a ubiquitous, highly negatively charged extracellular matrix polysaccharide involved in many biological processes. It is bound as a proteoglycan together with transmembrane or membrane-anchored proteins, forming the heparan sulfate proteoglycan (HSPG). The highly negatively charged environment may have a positive or negative influence on viral heparan sulfate binding proteins in order to reach the cell membrane for viral entry. To analyze the effect of heparan sulfate, the viruses and cells are incubated with various concentrations of heparan sulfate. After infection with special viruses, the luciferase assay is used to determine whether heparan sulfate has a positive or negative influence on the viral entry. Furthermore, an enzymatic digestion by heparinase I and III, as well as the change in sulfation with sodium chlorate, the cell surface is changed with respect to heparan sulfate. Here, a significant decrease in viral entry into the cell should be visible. The cell surface alteration is detected by various western blots, using antibodies like anti-syndecan-1 and anti-heparan sulfate. Overexpression by transfection of plasmids or down regulation by syndecan-1 shRNA could be further evidence for the involvement of heparan sulfate in the entry of HERV-K (HML-2).

By these two approaches on the one hand a specific entry of the virus by receptors is examined and on the other hand an interaction with glycosaminoglycan's on the host cell with certain binding proteins on the viral envelope. Because of the different methods, a broad experimental spectrum is available, which could provide accurate information on the entry of HERV-K (HML-2).

2. Material and Methods

2.1 Material

2.1.1 Equipment

TABLE 1: Device list

Equipment	Company
Balance	Sartorius, Göttingen, Germany
Balance PR803	Mettler Toledo, Ohio, USA
Biofuge Heraeus Prima R	Thermo Fisher Scientific, Schwerte, Germany
Centrifuge 4K15	Sigma Aldrich, Steinheim, Germany
Centrifuge 5415D	Eppendorf, Hamburg, Germany
Electrophoresis Chamber	Bio Rad, München, Germany
ELISA Reader Sunrise	Tecan Group, Männedorf, Switzerland
Fluorometer Qubit 3	Life Technologies, California, USA
Incubator Hera Cell 240	Thermo Fisher Scientific, Schwerte, Germany
Incubator Shaker C24	New Brunswick Scientific, New Jersey, USA
Luciferase Reader Centro LB960	Berthold Technologies, Bad Wildbad, Germany
Microscope Eclipse TS100	Nikon, Tokio, Japan
Multiskan GO	Thermo Fisher Scientific, Schwerte, Germany
Nanodrop 1000	peQLab, Erlangen, Germany
Odyssey	Li-Cor Biosciences, Nebraska, USA
pH Meter MP220	Mettler Toledo, Ohio, USA
Power Pac Basis and HC	Bio Rad, München, Germany
Thermo Stat Plus Shaker	Eppendorf, Hamburg, Germany
Thermomixer 5436	Eppendorf, Hamburg, Germany
Trans Blot SD	Bio Rad, München, Germany
Transilluminator GelDoc	Phase, Lübeck, Germany
Ultra-Low Freezer U57085	New Brunswick Scientific, New Jersey, USA
Ultracentrifuge Optima L-100K	Beckman Coulter, California, USA
Water Bath	Köttermann, Uetze/Hänigsen, Germany

2.1.2 Consumables

TABLE 2: List of consumables

Product	Company
6-well Plates	TPP, Trasadingen, Switzerland
96-well Plates for Cell Culture	TPP, Trasadingen, Switzerland
96-well Plates for ELISA	Thermo Fisher Scientific, Schwerte, Germany
96-well Plates for Luciferase Assay	Thermo Fisher Scientific, Schwerte, Germany
Cell Culture Dish 15cm	TPP, Trasadingen, Switzerland
Cell Culture Flask T75 and T150	TPP, Trasadingen, Switzerland
Cell Scrapers 24cm and 30cm	TPP, Trasadingen, Switzerland
Clip Tips	Thermo Fisher Scientific, Schwerte, Germany
Cryo.S Tubes	Greiner Bio-One, Kremsmünster, Austria
Falcon Tube 15ml and 50ml	TPP, Trasadingen, Switzerland
Filter Tips	Eppendorf, Hamburg, Germany
Pipette Tips	Thermo Fisher Scientific, Schwerte, Germany
Reaction Tubes 1.5ml and 2ml	Eppendorf, Hamburg, Germany
Serological Pipette	TPP, Trasadingen, Switzerland
Sterilcup and Steriltop	Merck, Darmstadt, Germany
Sterile Filter 0.45µm	Sartorius Stedim Biotech, Goettingen, Germany
Sterile Syringe Omnifix 50ml	Braun, Melsungen, Germany
Ultra-Clear Centrifuge Tube	Beckman Coulter, California, USA
X-ray Film	Kodak, Rochester, USA

2.1.3 Chemicals

TABLE 3: Chemicals that are not from the company Roth.

Product	Company
Albumin Standard 2mg/ml	Thermo Fisher Scientific, Schwerte, Germany
Ammonium Persulfate	Thermo Fisher Scientific, Schwerte, Germany
Carbonate-Bicarbonate Tablet	Sigma Aldrich, Steinheim, Germany
cOmplete Protease Inhibitor Cocktail	Sigma Aldrich, Steinheim, Germany
Dimethyl Sulphoxide Hybri-Max	Sigma Aldrich, Steinheim, Germany
DMEM High Glucose	Robert Koch Institut, Berlin, Germany
Ethidium Bromide Solution	Sigma Aldrich, Steinheim, Germany
FBS Superior S0615/0114G	Biochrome, Berlin, Germany
Glutamine 200mM	Biochrome, Berlin, Germany

Hams´s F12	Robert Koch Institut, Berlin, Germany
Heparan Sulfate 5mg	Sigma Aldrich, Steinheim, Germany
HIV-Standard 290ng/ml	Robert Koch Institut, Berlin, Germany
Hydrogen Peroxide Solution 30% (w/w)	Sigma Aldrich, Steinheim, Germany
LB Medium	Robert Koch Institut, Berlin, Germany
o-Penylenediamine Dihydrochloride 5mg	Sigma Aldrich, Steinheim, Germany
Penicillin/Streptomycin (P=10000U/ml and S=10000µg/ml)	Gibco by Life Technologies, California, USA
Phosphate-Citrate Tablet	Sigma Aldrich, Steinheim, Germany
Polyethylenimine, branched	Sigma Aldrich, Steinheim, Germany
RPMI 1640	Robert Koch Institut, Berlin, Germany
Separating Gel Buffer 1.5M Tris-HCL	Bio Rad, München, Germany
Stacking Gel Buffer 0.5M Tris-HCL	Bio Rad, München, Germany
Triton-X100	Sigma Aldrich, Steinheim, Germany
Trypsin (0.05%)/EDTA (0.02%) Solution	Biochrome, Berlin, Germany

2.1.4 Cell culture media

Dulbecco's Modified Eagle's Medium (DMEM)

1	x	DMEM High Glucose
10	% (v/v)	Fetal Bovine Serum (FBS)

RPMI 1640

1	×	RPMI 1640
10	% (v/v)	Fetal Bovine Serum (FBS)

Ham´s F12

1	×	Ham´s F12
10	% (v/v)	Fetal Bovine Serum (FBS)
4,0	mM	Glutamine

Freezing Medium

10	% (v/v)	DMSO
90	% (v/v)	Fetal Bovine Serum (FBS)

2.1.5 Buffers and solutions

Tris-NaCl-EDTA Solution (TNE)

10	mM	Tris	
1	mM	EDTA	
100	mM	NaCl	pH 7.5

50× Tris Acetat EDTA Buffer (TAE)

2	M	Tris base	
250	mM	Sodium acetate	
60	ml/l	Acetic Acid	
50	mM	EDTA	pH 7.8

Heparinase I Buffer

20	mM	Tris-HCL	
50	mM	NaCL	
4	mM	$CaCl_2$	
0.01	%	BSA	
	in	Aqua dest.	pH 7.5

Heparinase III Buffer

20	mM	Tris-HCL	
4	mM	$CaCl_2$	
0.01	%	BSA	
	in	Aqua dest.	pH 7.5

For Western Blot Analysis

NP-40 Cell Lysis Buffer

50	mM	Tris-HCL	
150	mM	NaCl	
1	%	NP-40	
1	x	Protease inhibitor	pH 8.0

RIPA Lysis Buffer

50	mM	Tris-HCL	
150	mM	NaCl	
0.1	%	SDS	
0.5	%	Sodium Deoxycholate	
1	%	NP-40 (or Triton X-100)	
1	x	Protease inhibitor	pH 8.0

10x Tris-Glycine Buffer

30.3	g/l	Tris
144.1	g/l	Glycine
to 1	l	Aqua dest.

Transfer Buffer

100	ml	10x Tris-Glycine Buffer	
200	ml	Methanol	
to 1	l	Aqua dest.	

PBS-T

0,001	%	Tween-20	
	in	1x PBS	

Blocking Solution

50	g/l	Milk powder	
	in	Aqua dest.	

10x Running Buffer

30.3	g/l	Tris	
144.1	g/l	Glycine	
10	g/l	Sodiumlaurylsulfate (SDS)	
	in	Aqua dest.	pH 8.3

Lämmli Buffer

20	g/l	SDS	
50	ml/l	B-Mercaptoethanol	
250	ml/l	Glycerol	
125	ml/l	Stacking Buffer	
0,01	%	Bromphenolblue	
	in	Aqua dest.	pH 6.8

6x DNA Loading Buffer

60	% (v/v)	Glycerol	
0.2	% (w/w)	Orange G	
60	mM	EDTA	pH 7.6

12% Stacking Gel

7.9	ml	Aqua dest.
9.6	ml	30% Acrylamide
6	ml	1.5M Tris
240	µl	10% SDS
240	µl	10% APS
24	µl	TEMED

4% Stacking Gel

8.9	ml	Aqua dest.
2	ml	30% Acrylamide
3.75	ml	0.5M Tris
150	µl	10% SDS
150	µl	10% APS
15	µl	TEMED

For p24 ELISA

Carbonate/Bicarbonate Buffer

1	Tabl.	Carbonate/Bicarbonate
100	ml	Aqua dest.

Phosphate/Citrate Buffer

1	Tabl.	Phosphate/Citrate
100	ml	Aqua dest.

Blocking Buffer

2	%	milk powder
1	x	1x PBS

Tween Solution

2	%	milk powder
0,05	%	Tween-20
1	x	1x PBS

Substrate Solution

5	mg	OPD
12	µl	30% H_2O_2
12,5	ml	Phosphate/Citrate Buffer

2.1.6 Cell lines

TABLE 4: used cells

Cells	Origin	Medium	Place in N
COLO 205	Colon	RPMI	T1, To2, B4, L7
HCT 116	Colon	RPMI	T1, To2, B4, L4 (1-5)
HEK 293T	Kidney	DMEM	T1, To2, B4, L2
Sk-Mel 28	Melanoma	DMEM	T1, To2, B4, L5 (1-5)

T…Tank, To…Tower, B…Box, L…Line

2.1.7 Antibodies

TABLE 5: used antibodies

Antibody	Species	Concentration	Company
Anti-Flag	Mouse (M)	1:1000	Sigma Aldrich, Steinheim, Germany
Anti-GAPDH	Rabbit (M)	1:5000	Biolegend, California, USA
Anti-HA	Mouse (M)	1:1000	Biolegend, California, USA
Anti-HA	Mouse (M)	1:1000	Cell Signaling, Massachusetts, USA
Anti-Heparan Sulfate	Mouse IgM (P)	1:200	Amsbio, Abingdon, UK
Anti-His	Mouse (M)	1:1000	Sigma Aldrich, Steinheim, Germany
Anti-p24	Mouse (M)	1:250	Sigma Aldrich, Steinheim, Germany
Anti-Syndecan-1 (A-6)	Mouse (M)	1:200	Santa Cruz, California, USA
Anti-V5	Mouse (M)	1:5000	Bio Rad, München, Germany
Coating Ab AG3.0	Human	1:1000	RKI, Berlin, Germany
HIV Poolserum (First Ab)	Human	1:5000	RKI, Berlin, Germany
Sec.Ab IRDye 680T	Goat Anti-Mouse (P)	1:20000	Li-Cor Biosciences, Nebraska, USA
Sec.Ab IRDye 800CW	Goat Anti-Mouse (P)	1:10000	Li-Cor Biosciences, Nebraska, USA

M…monoclonal, P…polyclonal

2.1.8 Kits

TABLE 6: List of used kits

Product	Company
One Shot Top10	Thermo Fisher Scientific, Schwerte, Germany
Pierce BCA Protein Assay Kit	Thermo Fisher Scientific, Schwerte, Germany
Plasmid Maxi Kit (25)	Qiagen, Hilden, Germany
Qubit 3 Reagents	Life Technologies, California, USA
RT Activity Kit	Cavidi, Uppsala, Switzerland

2.1.9 Ready reagents

TABLE 7: used ready reagents

Product	Company
Loading Dye 6x	Thermo Fisher Scientific, Schwerte, Germany
GeneRuler™ 1 kb DNA Ladder	Thermo Fisher Scientific, Schwerte, Germany
GeneRuler™ 1 kb+ DNA Ladder	Thermo Fisher Scientific, Schwerte, Germany
GeneRuler™ 100 bp+ DNA Ladder	Thermo Fisher Scientific, Schwerte, Germany
Gold Protein Marker IV	peQLab, Erlangen, Germany
Page Ruler Prestained Protein Ladder	Thermo Fisher Scientific, Schwerte, Germany
Passive Lysis Buffer 5x	Promega, Madison, USA
Phosphate Buffered Saline (PBS)	Robert Koch Institute, Berlin, Germany
Rapid Detection of Firefly Luciferase	Promega, Madison, USA

2.1.10 Enzymes

TABLE 8: List of the used enzymes

Product	Company
BamH I	New England Biolabs, Massachusatts, USA
Bgl II	New England Biolabs, Massachusatts, USA
Heparinase I - 50U	Sigma Aldrich, Steinheim, Germany
Heparinase III - 10U	Sigma Aldrich, Steinheim, Germany
Hind III	New England Biolabs, Massachusatts, USA
NotI	New England Biolabs, Massachusatts, USA
Pstl I	New England Biolabs, Massachusatts, USA
SaC I	Thermo Fisher Scientific, Schwerte, Germany
Xma l	New England Biolabs, Massachusatts, USA

2.1.11 Plasmids

TABLE 9: used plasmids

Plasmid	Concentration in ng/µl	Description
BC-GPR56	1006	G-protein coupled receptor 56
CD63-pEGFP-C2	1070	Lysosomal-associated membrane protein 3
Env Syncytin-1 V5-Tag	2900	Viral envelope for Syncytin-1
Env Syncytin-2 V5-Tag	2800	Viral envelope for Syncytin-2
GPR161-Tango	984	G-protein coupled receptor 161
GPR56 (ADGRG1)	728.5	G-protein coupled receptor 56
MMTV-Co-Env-V5	1052	Viral envelope for MMTV
orico env Δc1	1943	Viral envelope for HERV-K
orico env Δc1 (R140C)	1739	Viral envelope for inactive HERV-K
pcAG NL1 (-)	1017	Neurologin-1 receptor
pCMV-VSV-G Myc	1684	Viral envelope for VSV-G
pCMV-VSV-G-Mut (P127D)	755	Viral envelope for inactive VSV-G
phL1A pcDNA3 (L1CAM)	1040	Neural cell adhesion molecule L1
pLVX-MFSD2A-myc	2567	Receptor for syncytin-2
psPAX2	1613	2nd generation lentiviral packaging plasmid
pWPXL-GFP	2024	2nd generation lentiviral transfer plasmid
Sc-36587-SH	100	Syndecan-1 shRNA
SLC1A4 (=ASCT1)	2100	Receptor for syncytin-1
SLC1A5 (=ASCT2)	1800	Receptor for syncytin-1
SORT1-bio-His	1056	Sortilin-1 receptor

2.1.12 HIV pseudotyped viruses

TABLE 10: produced pseudotyped HIV´s

Virus	P24 Concentration in ng/µl
HERV R140C	11.07
HERV Δc1	30.87
Syncytin-1	12.41
Syncytin-2	0.77
VSV-G	19.11
VSV-Mut	23.5

2.2 Methods

2.2.1 Cell biological methods

2.2.1.1 General culture conditions

As described in table 4, all cells were cultured in DMEM or RPMI with 10% FCS and 50 U/ml penicillin and 50µg/ml streptomycin under standard cell culture conditions (37°C, 5% CO_2) in cell culture flask. Furthermore, the cell culture conditions in this work were adapted to the use of sodium chlorate. For this purpose, several preliminary tests were carried out to allow a proper use of sterile sodium chlorate.

TABLE 11: plated cell number for different dishes and plates

	cell number
10cm dish	$4x10^6$ cells/dish
15cm dish	$9x10^6$ cells/dish
96-well plate	$1.2x10^4$ cells/well
6-well plate	$5x10^5$ cells/well

2.2.1.2 Determination of the cell number

To count the cells 10 µl of the resuspended cells were transferred to a Neubauer counting chamber and four large squares were counted in a meandering fashion.

$$\frac{\boldsymbol{counted\ cells}}{\boldsymbol{number\ of\ large\ squares}} \times \mathbf{10^4}\ (\boldsymbol{chamber\ factor}) \times \boldsymbol{dilution} = \boldsymbol{x\ cells/ml}$$

2.2.1.3 Trypsinization of adherent cells

To detach the cells from the bottom of the cell culture flask, the medium was aspirated and the cells were washed with PBS. After addition of 2ml of trypsin/EDTA and an incubation time of 5 minutes at 37°C, the cells dissolved and could be gently and continuously resuspended in 8ml of medium so that cell aggregates were dissolved. This cell suspension was used for sub culturing as well as for experiments.

2.2.1.4 Centrifugation

Unless otherwise described, cells were centrifuged at room temperature and 300 x g for 5 minutes.

2.2.1.5 Thaw and freeze of cells

In order to ensure a long-term use of a cell lines, a part of this after re-thawing and about two times passaging was frozen again. For this purpose, the excess of cells after passaging once washed in PBS and centrifuged. The cell pellet of a 75cm² cell culture flask was then resuspended in a certain volume of freezing medium. Of these, 1ml with $1x10^6$ cells were transferred in a cryotube and cooled down slowly to -80°C over a period of 24 hours with an isopropanol-filled freezing container in order to ensure cell-friendly freezing. The storage of the cell lines took place permanently in a tank with liquid nitrogen at -196°C. To thaw cells stored in liquid nitrogen, they were gently warmed in a water bath at 37°C and resuspended in 5ml of complemented DMEM. After pelleting the supernatant was discarded and the cell pellet resuspended in 12ml of the right medium. The further cultivation was carried out as described in section 2.2.1.1. The freezing and thawing of cell lines was under sterile conditions.

2.2.1.6 PEI transfection

In transfection, plasmid DNA is transiently or permanently introduced into eukaryotic cells by various methods. The transfection of the cells was carried out at the earliest one day after seeding in the culture vessel in order to ensure a good adherence of the cells to the bottom. The cells showed a spreading morphology and a confluence of 50-80%.

Polythylenimine is a stable cationic polymer and condenses DNA into positively charged particles that bind to anionic cell surfaces. Consequently, the DNA:PEI complex is endocytosed by the cells and the DNA released into the cytoplasm (Sonawane *et al.*, 2003).

Prior to transfection bring all reagents to room temperature. In a sterile tube dilute total plasmid DNA in serum-free DMEM (volume is 10% of the final volume of the culture vessel). By viral production use a plasmid ratio of 4:3:1 (Backbone:Packaging:Envelope). Add PEI to the diluted DNA and mix immediately by vortexing or pipetting. The volume of used PEI is based on a 3:1 ratio of PEI (µg):total DNA (µg). After an incubation time of 15 minutes at room temperature add the DNA/PEI mixture dropwise to the rest of the medium (can contain antibiotics) with adherent cells. After 8-24 hours the PEI/DNA mixture can be replaced with fresh medium. Harvest transfected cells or viral supernatants at 48 hours post-transfection. Every transfection was checked with a specific plasmid that generated a GFP signal and could be examined under a microscope.

TABLE 12: PEI transfection protocol per well

	DNA	PEI (2.5µg/µl)	Medium
96-well plate	0.1µg	0.12µl	20µl
6-well plate	3µg	3.6µl	200µl
15 cm dish	12µg	14.4µl	2000µl

2.2.1.7 Viral infection

For the entry experiment, cells were seeded in 96-well plates and cultured for 24 hours. Thereafter, the medium was removed and overlaid with 50ul of new medium. This medium contained the virus with a p24 concentration of 100ng per well. Due to the high infection rate of VSV, only 1ng / well virus was used. After a one-hour incubation at 37 ° C, the viral medium was removed, the cells washed with PBS and cultured for an additional 48 hours under standard cell culture conditions. During this time, the luciferase could be formed, which was then quantified.

2.2.1.8 Production of viral stocks

To prepare viral stocks, the supernatant was removed from various 15 cm dishes after transfection and sterile filtered with a 0.45 µm filter. This will remove any cell debris and leave only the smallest components in the medium. For purification, 5ml of 20% sucrose was placed in an Ultra Clear Centrifuge tube and carefully pipetted about 30 ml supernatant on it, resulting in two phases. After ultra-centrifugation at 32,000 RPM for 3 hours at 4°C, the medium was decanted and the pellet resuspended in about 200-300 µl 1xPBS. The viruses were stored after aliqouting at -80°C.

2.2.1.9 Incubation with heparan sulfate

In order to analyze the occurrence of viruses by means of heparan sulfate proteoglycans, cells and viruses were incubated with different concentrations of heparan sulfate and after this the viral entry inside the cells was examined. For this experiment, cells were seeded in a 96-well plate and cultured for 24 hours at standard cultivation conditions. Thereafter, the viruses were incubated for one hour at 37°C with four different concentrations of heparan sulfate (HS). For this, 50 µl HS and 50 µl virus were mixed, resulting in a concentration of 400 µg/ml, 200 µg/ml, 100 µg/ml and 50 µg/ml. After this one-hour incubation, the HS/virus mixture was added to the cells and stored for a further hour at 37°C. Thus, the cells were incubated with 100ng of virus (1ng for VSV-G) and a certain concentration of HS. After the solution was removed and the cells were washed with 1xPBS, they were cultivated for another 48 hours before being processed for the luciferase measurement.

2.2.1.10 Cultivation with sodium chlorate

Cells were cultivated for more than 2 passages with low sulfated Ham´s F12 growth medium and 25mM, 50mM and 100mM sodium chlorate. Fresh sodium chlorate was added to each medium change. After the long-time incubation the cells were seeded in 96-well plates with the same medium and 24 hours later incubated with 100ng virus (1ng for VSV-G). After the solution was removed and the cells were washed with 1xPBS, they were cultivated for another 48 hours before being processed for the luciferase measurement.

2.2.1.11 Enzymatic digestion with heparinase I and III

For this experiment, cells were seeded in a 96-well plate and cultured for 24 hours at standard cultivation conditions. The heparinase I and III (blend) was dissolved in Hep.I buffer and the concentrations of 0.00001mU/ml, 0.01mU/ml and 10mU/ml were adjusted. In order to allow an optimal reaction, the cells were incubated with in each case 50µl heparinase in Hep.I buffer (without medium) for one hour at 37°C, since a precise pH value is necessary in enzymatic reactions. After the solution was removed and the cells were washed with 1xPBS, they were cultivated for another 48 hours in standard medium before being processed for the luciferase measurement.

2.2.1.12 Creation of growth curves

To analyze the proliferation behavior of the cell line SK-Mel28 with sodium chlorate, growth curves were generated. For this purpose, a defined number of 6-well plates were seeded in parallel and counted at certain times over a certain period of time.

For this experiment, three cell culture flask were trypsinized, the cell suspension pooled and the cells counted to determine the number of cells per ml. For each batch, cells were seeded into two 6-well plates with a cell number of $4x10^4$ cells and incubated for 12 days at standard cell culture conditions. Every second day the medium was changed with fresh sodium chlorate. One well of each condition (table 14) was trypsinized and counted every day in a defined volume. The values obtained were plotted logarithmically, which makes it possible to determine the latency phase, exponential phase, stationary phase and dying-off phase. The population doubling time (PDT) was determined by the following formula:

$$\frac{\boldsymbol{ln\,2}}{\boldsymbol{ln}\left(\frac{\boldsymbol{cell\ number\ t2}}{\boldsymbol{cell\ number\ t1}}\right)} \times (\boldsymbol{t2} - \boldsymbol{t1}) = \boldsymbol{PDT}$$

TABLE 13: Different conditions for the growth curves with sodium chlorate in Ham´s F12 medium

Conditions	Composition
1	0 mM $NaClO_3$
2	25 mM $NaClO_3$
3	50 mM $NaClO_3$
4	100 mM $NaClO_3$

2.2.1.13 shRNA transfection

To silence target gene expression via RNA interference a short hairpin RNA was used. It´s an artificial RNA molecule with a tight hairpin turn, which binds to a specific RNA of the cell and blocks the translation procedure.

To get the shRNA expression into the cell, the specific plasmid was delivered by PEI transfection. For this, a 6-well plate was seeded with cells and after 24 hours transfected with 1µg and 2µg shRNA (table 15). To select the stable transfected cells from non-transfected cells the antibiotic puromycin was used in a cell specific concentration, because the plasmids have coded a puromycin resistant section. To select a specific puromycin concentration for HEK293T and SK-Mel28, a puromycin kill curve was created. For those two 6-well plates for each cell line was seeded and after 24 hours incubated with different concentrations puromycin. There was used the concentrations from 0-5µg/ml and incubated for 2 weeks. During this time every second day the medium was changed with fresh antibiotics and the minimal concentration at which the non-transfected cells died was used for the assay.

For HEK293T a concentration of 1.5µg/ml and for SK-Mel28 a concentration of 1µg/ml was used. After a selection and cultivation for 1-2 weeks to get a larger amount of transfected cells, a 96-well plate was seeded and 24 hours later incubated with 100ng virus (1ng for VSV-G). After the solution was removed and the cells were washed with 1xPBS, they were cultivated for another 48 hours before being processed for the luciferase measurement.

TABLE 14: PEI transfection protocol per well for shRNA

shRNA	DNA	PEI (2.5 µg/µl)	Medium
Syndecan-1	1µg	1.2µl	200µl
	2µg	2.4µl	200µl
Fibronectin	1µg	1.2µl	200µl
	2µg	2.4µl	200µl

2.2.2 Protein analytics

2.2.2.1 P24 capture ELISA

The p24 antigen capture ELISA is used to detect the Gag antigen of the HI virus.

In the first step, the 96-well plate had to be coated with the monoclonal antibody AG 3.0. Since the production of the antibody takes place internally, each time the best concentration in tested for coating with an antigen standard. For coating the plate, the antibody was diluted in 5 ml of carbonate/bicarbonate buffer and 50µl was added to each well. The plate was stored in the fridge at 4°C overnight for incubation. The next day, the plate was washed three times with 1xPBS and the remaining binding sites on the plate were blocked by adding 100µl of blocking buffer to each well for 30 minutes at 37°C. After incubation, the plate was washed again and the samples applied. The samples were the inactivated (with a final 0.2% Tween concentration) viruses. For this purpose, a 1:3 dilution series with buffer and samples was created on the plate and incubated again by 37°C for one hour. During the incubation period, the primary antibody was prepared, which was an HIV-1^+ plasma pool serum and diluted 1:5000 in PMT. After adding of 50µl and a further incubation for one hour at 37°C the secondary antibody the plate was washed again three times with 1xPBS. The secondary HRP linked antibody was diluted 1:1000 with PMT, added (50µl/well) and incubated for 1 hour at 37°C. 50µl of the OPD-substrate solution was added after the last washing step with 1xPBS and then incubated for 10 minutes at room temperature. To stop the reaction and get the final color signal, 25µl of a 5% H_2SO_4 solution was added. Subsequently, the samples were measured by means of Tecan Sunrise reader and analyzed. To prepare a standard curve for the final calculation, a sample with a known concentration (290ng/ml) was carried.

2.2.2.2 Measurement of the luciferase activity

In the luciferase assay, reporter constructs carrying a firefly luciferase gene behind a CMV promotor and after this, the sequence which is important to produce virus particles. The luciferase catalyzes a reaction in which light is emitted whose intensity is proportional to the amount of produced firefly luciferase. This allows conclusion to be drawn about the rate of synthesis of HERV-K virus like particles. For infection experiments, cells were incubated for one hour at 37°C with viruses which have the luciferase construct. After this step the cells were washed with PBS and cultivated with the standard growth medium at 37°C. 48 hours after infection, the cells were lysed with 200µl 1x Passive Lysis Buffer according to the manufacturer. 20µl of the lysate were pipetted into a white 96-well luminometer plate and the light intensity was measured after a 10 seconds delay with the Berthold Centro LB 960 luminometer. This device automatically injected 50µl of the firefly luciferase substrate into each well.

2.2.2.3 SDS-Polyacrylamide gel electrophoresis (SDS-Page)

The SDS-Page is a method for separating denatured proteins by size in the electric field (LAEMMLI, 1970). Sodium dodecyl sulfate (SDS) leads to denaturation of proteins and covers their own charge. Thus, all SDS-loaded proteins get a negative charge and, due to their unequal size, migrate in the gel at different rates and under the influence of the electric field thus separated. 4% stacking gels and 12% running gels (table 16) with a thickness of 1.5mm were used, the concentration of the separation gel depending on the size of the proteins to be separated. The smaller the protein to be separated, the higher should be the separating gel. The optimum range of rotation of 12% running gels is 72kDa to 34kDa. The wide-pored, stacking gel preceded by the separating gel accounts for about one quarter of the total gel and serves to concentrate the sample at the boundary layer of the two gels. Thus, the sample penetrates into the running gel as a very thin band and can be separated in a clearly structured manner. The components of the gels are blended together, with ammonium persulfate (APS) and N, N, N', N'-tetramethylethylendiamine (TEMED) catalyzing the crosslinking of the acrylic monomers. Before applying the protein samples, they were isolated from fresh cultivated cells with RIPA-buffer for 10 minutes on ice. After a centrifugation with 15,000 RPM for 10 minutes the protein concentration of the supernatant was analyzed by Pierce BCA Protein Assay Kit from Thermo Fisher (proceed as described by the manufacturer). Before applying the samples, they treated with the same volume of 6x Laemmli sample buffer and 5% β-mercaptoethanol and denatured for 10 minutes at 95°C in a heating block. The hydrogen bonds of the tertiary and secondary structures are broken up by the SDS and the disulfide bridges are reduced by β-mercaptoethanol. The concentration of the samples and the size standard in the stacking gel was carried out at 100V until the running front passed through the boundary layer to the running gel. The voltage was increased to 120V to separate the samples until the run front started to run out of the gel after about 90 minutes. This was followed by Western Blot analysis as described in the next section.

TABLE 15: Composition of 3 stacking and running gels

Components	4% Stacking Gel	12% Running Gel
ddH_2O	8.9ml	7.9ml
30% Acrylamide	2ml	9.6ml
0.5M Tris pH 6.8	3.75ml	6ml
10% SDS	150µl	240µl
10% APS	150µl	240µl
TEMED	15µl	24µl
Total Volume	15ml	24ml

2.2.2.4 Western Blot analysis

The size-separated proteins were transferred to a nitrocellulose membrane in the Western Blot and subsequently identified and quantified using specific antibodies. First, the tailored membrane with a pore of 0.45µm and SDS gel was washed in transfer buffer for at least 20 minutes. After this, the protein transfer was done by semi-dry blotting procedure. For this, the gel was placed on the membrane between two blotting papers soaked in transfer buffer and blotted for 45 minutes at 15V. Subsequent pivoting of the membrane in milk powder buffer overnight blocked non-specific antibody bindings. Incubation of the primary antibody (which was diluted in PBS-T) was for one hour at room temperature or overnight at 4°C. After washing three times in PBS-T for five minutes each, the membrane was incubated with fluorescent labeled secondary antibody, which was also diluted in PBS-T, for one hour at room temperature in the dark. After another washing step with PBS-T, the fluorescence signal was evaluated on the Odyssey Infrared Imaging System.

2.2.3 Molecular biological methods

2.2.3.1 Transformation

The transformation of the plasmids was carried out by means of One Shot™ Top10 chemically competent E. coli. The protocol “Chemical transformation procedure” from the manufacturer was used for the experiments. Part of the transformation mixture was then plated on LB agar selection plates supplemented with ampicillin or kanamycin.

2.2.3.2 Plasmid cloning and isolation

For the cloning of plasmids “One Shot Top10” were transformed with these, shaken and plated out, as already described in the previous section. The next day, the single colonies were transferred to 2ml LB medium supplemented with ampicillin or kanamycin and shaken at 37°C and 250rpm for 4-8 hours. This 2ml day-culture was transferred to 2 2L baffled flask with 250ml LB medium and shaken overnight under the same condition. The subsequent plasmid isolation was carried out according to the manufacturer´s instructions by means of Plasmid Maxi Kit (25). The DNA was diluted in 200µl distilled water and the concentration determined by NanoDrop1000 (table 9).

2.2.3.3 Glycerol stock

In order to accelerate the cloning process for commonly used plasmids glycerol stocks were made. 500µl of the bacterial solution were taken from the overnight culture before starting the plasmid isolation, mixed together with 500µl of 95% glycerol and stored at -80°C. For future plasmids preparations, a pipette tip was dipped briefly in the glycerol stock and placed in the 2ml LB medium and shaken at 37°C and 250rpm.

2.2.3.4 DNA quantification

The DNA quantification was carried out with a NanoDrop1000 according to the manufacturer, at a wavelength of 260nm and 280nm. For the absorption measurement of the DNA, 1µl of the eluted DNA was used. To make a statement about the purity of the DNA, the coefficient was calculated from the optical density at 260nm and 280nm. The highly purified DNA had a barely measurable protein concentration, which was reflected in a coefficient of 1.8 to 2.0.

2.2.3.5 Restriction with endonucleases

For verification of vectors and for cloning, the DNA was digested with specific bacterial restriction endonucleases (table 8). They each recognize one specific palindrome-like sequence within the DNA and produce there ends with 5’ overhang. The various type II restriction endonucleases were added to the DNA for approximately one hour at 37°C. To analyze the restriction digest were the mixtures are checked by DNA agarose gel electrophoresis.

Approach – Digestion: 1000ng Plasmid
2.5µl Endonuclease Buffer
1µl Endonuclease
add. to 25µl Aqua dest.

2.2.3.6 DNA agarose gel electrophorese

DNA agarose gel electrophoresis as a standard method is used to control, identify and purify nucleic acids by size and charge. The agarose powder was boiled with 1xTAE buffer to 0.8-1.5% agarose solution, depending on the size of the DNA to be separated. For this work, 0.8% agarose gels were used and 0.5µg/ml ethidium bromide was added. Ethidium bromide binds to the DNA during separation in the electric field, thus allowing visualization under UV light. Before applying the samples, they were spiked six times with 6x DNA loading dye and separated at a voltage of 90V in an electric field. The status of the sample separations could be tracked by means of Orange-G in the DNA loading dye. By carrying a size standard, a sizing and assignment of the fragments was possible. The documentation of the agarose gel was carried out under UV light at a wavelength of 302nm using Transilluminator GelDoc.

3. Results

3.1 Viral entry by transfection of specific receptors

3.1.1 The effect of the HERV envelope proteins syncytin-1 and syncytin-2 for cell fusion

To carry out the receptor expression experiments, the epithelial cell line HEK293T was used. After transfection of the receptors ASCT1 and ASCT2 for syncytin-1 and MFSD2A for syncytin-2, morphological changes on the cell line could be observed after 24 hours. Not only a reduction in the number of cells, but also a slight clumping of the cells in the monolayer was evident.

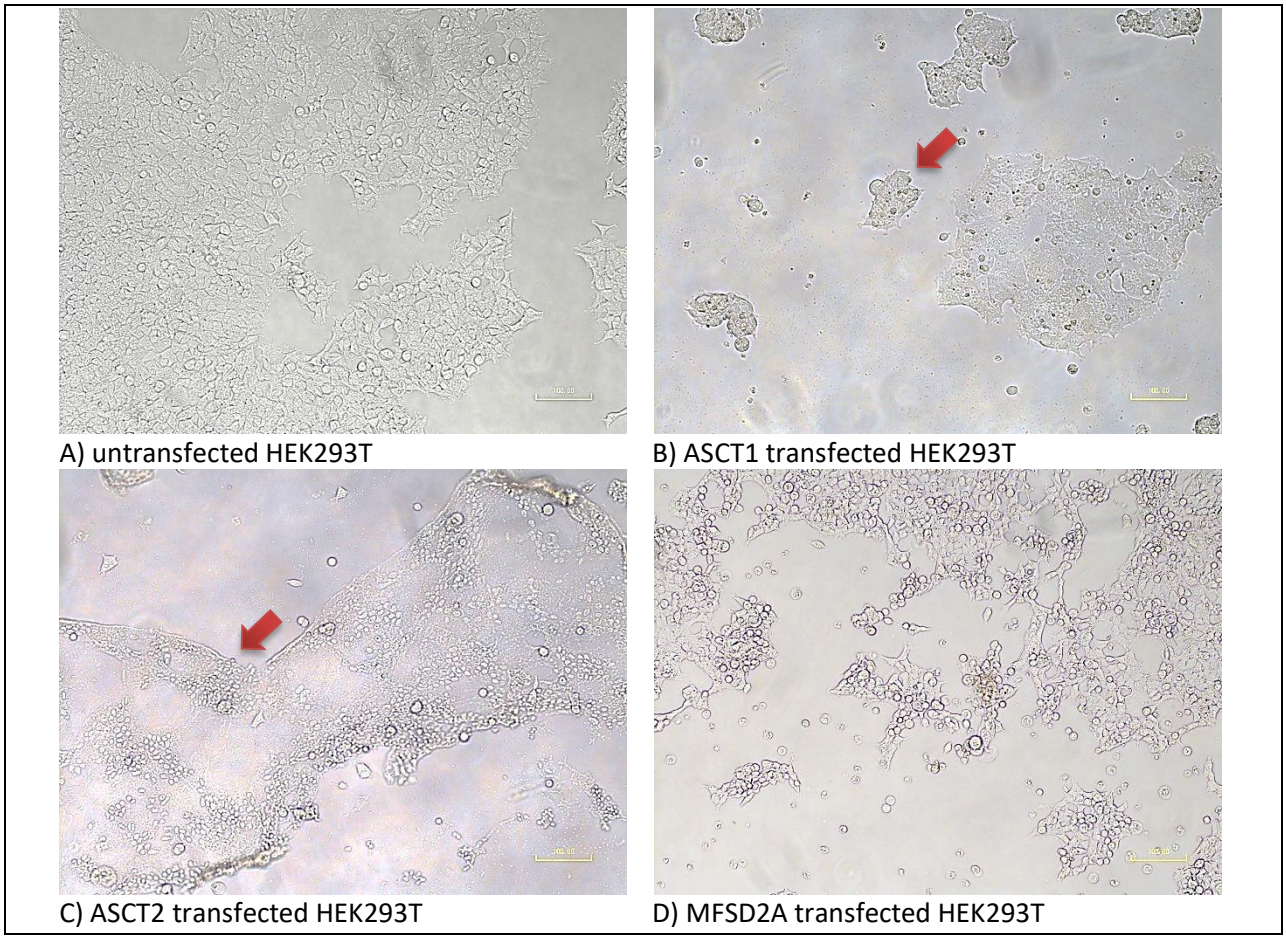

Figure 8: Differences in the morphology and growth behavior of HEK293T in the monolayer with different receptor transfections

After transfection with different plasmids, some of the cells died and others fused easily to the membrane. The reason for this was the formation of receptors for syncytin-1 (B and C). While the untransfected cell line (A) had a cobblestone-like structure, no clear cell structure could be detected in the cells with ASCT1 and ASCT2 (red arrows). The cells with the receptor for syncytin-2 (D) formed long cytoplasmic shoots and an increase in cells in the mitotic phase. Measuring bar= 100µm; Magnification= 100x

For this entry experiment, pseudotyped HI viruses with a HERV-K (Δc1), VSV-G, syncytin-1 and syncytin-2 envelope and a luciferase activity were prepared. After transfection with the specific receptors and infection with the pseudotyped viruses, the luciferase activity was measured and evaluated in the diagrams in figure 8. The untransfected HEK293T cells were considered to 100% and the infection of the transfected cells was normalized to these. The left diagram clearly shows that a simultaneous transfection with ASCT1 and ASCT2 has reached the highest infection rate for the control syncytin-1. Here a 17-fold higher infection could be determined, as if the receptors were transfected individually. Also in the right diagram, the syncytin-2 pseudotyped HI virus infected the MFSD2A transfected HEK293T cells 8-fold more. The other control infection with the VSV-G viruses showed a constant infection rate in every condition. Based on these control infections, it can be said that the receptors have no influence on the entry of Δc1 pseudotyped HI viruses into the ASCT1/2 and MFSD2A transfected cells. None of the infections with Δc1 shows an increased infection rate, as this is even lower than in the untransfected cells.

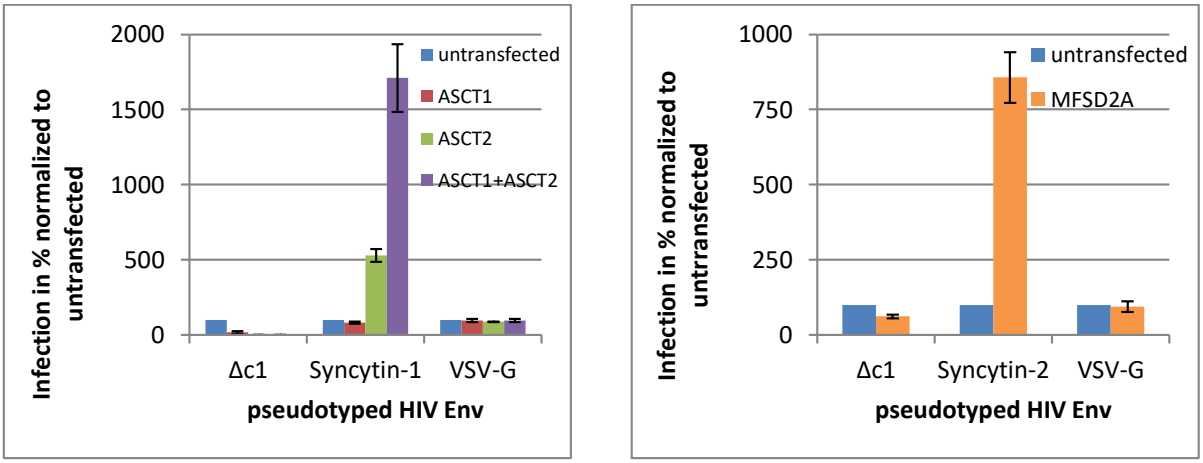

Figure 9: Infection of pseudotyped HI viruses of ASCT1/2 and MFSD2A transfected HEK293T cells
On the left side you can see the infection of ASCT1 and ASCT2 transfected HEK293T cells with HERV-K (Δc1) pseudotyped HI viruses. An infection with syncytin-1 pseudotyped viruses of ASCT1 and ASCT2 transfected cells has a 17-fold higher possibility to enter the cell, than untransfected cells. The right diagram shows the infection rate of HERV-K (Δc1), syncytin-2 pseudotyped HI viruses to MFSD2A transfected HEK293T cells. The values were normalized to the untransfected cell line, which was set to 100%. The non-functional virus mutants R140C and VSV-mutant, as well as the PBS control (mock), did not show luciferase activity after infection. Due to the biological replicates a standard deviation was determined.

To evaluate the data, a western blot was used to check if the receptors were expressed on the cell surface. Since the transfected plasmids had a Myc- and Flag-tag, the expression could be detected by means of specific antibodies. The blot was evaluated by fluorescence labeled antibodies and Flag was shown in green and GAPDH in red. As can be seen GAPDH was detected at about 37kDa and ASCT1/2 at 55kDa and MFSD2A at about 60kDa. Since the untransfected cells have no Flag-tag, it can be assumed that the transfection of the receptors in HEK293T cells was successful.

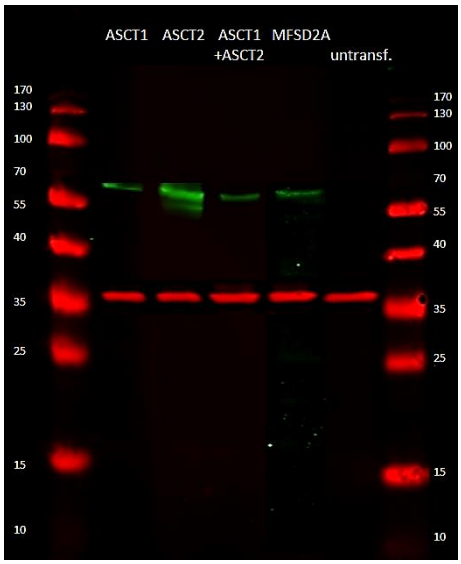

Figure 10: Western Blot of ASCT1/2 and MFSD2A transfected HEK293T cells with Flag and GAPDH antibodies

The Blot shows the expression of GAPDH (red) and the Flag-tag (green) of ASCT1/2 and MFSD2A. The markers on the left and right side provide information on the approximate size of the proteins sought from 10kdA to 170kDa. The samples from left to right are ASCT1, ASCT2, ASCT1 + ASCT2, MFSD2A and untransfected HEK293T cells.

3.1.2 Transfection of receptor candidates for specific HERV-K (HML-2) entry

To confirm the exact receptor responsible for HERV-K (HML-2) entry, several receptor candidates were transfected into the HEK293T cell line. After infection with HERV-K pseudotyped HIV and various control viruses, the luciferase activity was measured and evaluated in the following diagram. The luciferase activity shows that none of the receptors used improved the entry of the virus Δc1. Only the HEK293T cells with transfected g-protein coupled receptor 56 showed a significant increase in the entry of Δc1 into the cell. The virus infected the cells with the GPR56 cells without this receptor. Due to the strong potential for infection of VSV-G only 1ng virus was used. VSV-G showed a consistent ability to infect all samples.

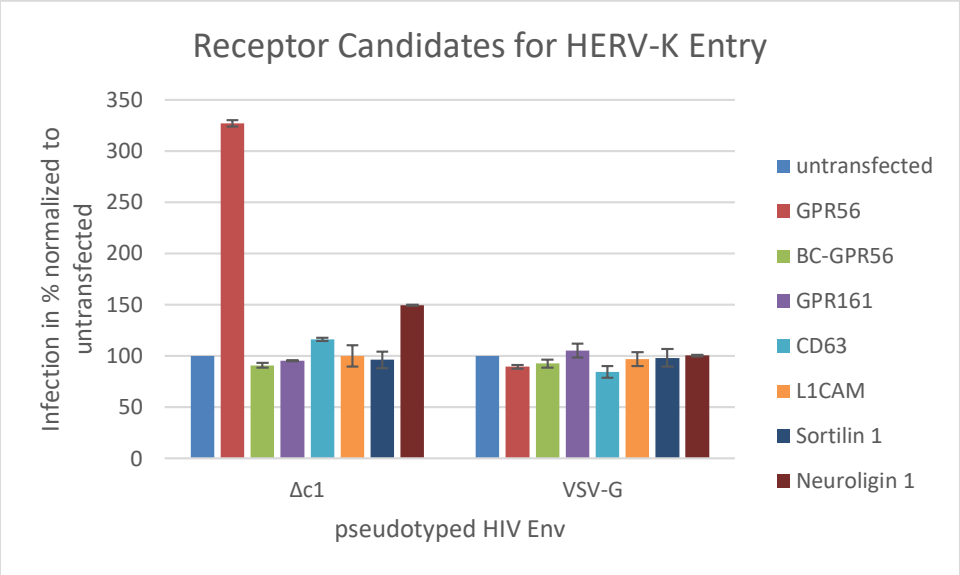

Figure 11: Luciferase Activity after infection of HEK293T cells with specific receptor candidates

The diagram shows the luciferase activity of the pseudotyped HI viruses used for the infection. The activity of the viral infection of the untransfected cells was set to 100% and the rest was normalized to this. HEK293T cells were transfected with 2 different types GPR56, as well as GPR161, CD63, L1CAM, sortilin 1 and neuroligin 1. The non-functional virus mutants R140C and VSV-mutant, as well as the PBS control (mock), did not show luciferase activity after infection. Due to the biological replicates a standard deviation was determined.

To verify that the receptors were expressed on the cells, lysates of the HEK293T cell line were checked by western blot analysis. Due to the different tags expression could be detected with the help of suitable antibodies. This revealed that all of the detectable receptors were expressed in the cells. The detection of neuroligin 1 was not possible due to the non-specific antibody binding and should possibly be repeated. Likewise, L1CAM and BC-GPR56 could not be tested because they did not have a tag and a specific antibody was not present. Since the receptor CD63 had an EGFP-tag, it could be detected by fluorescence microscopy.

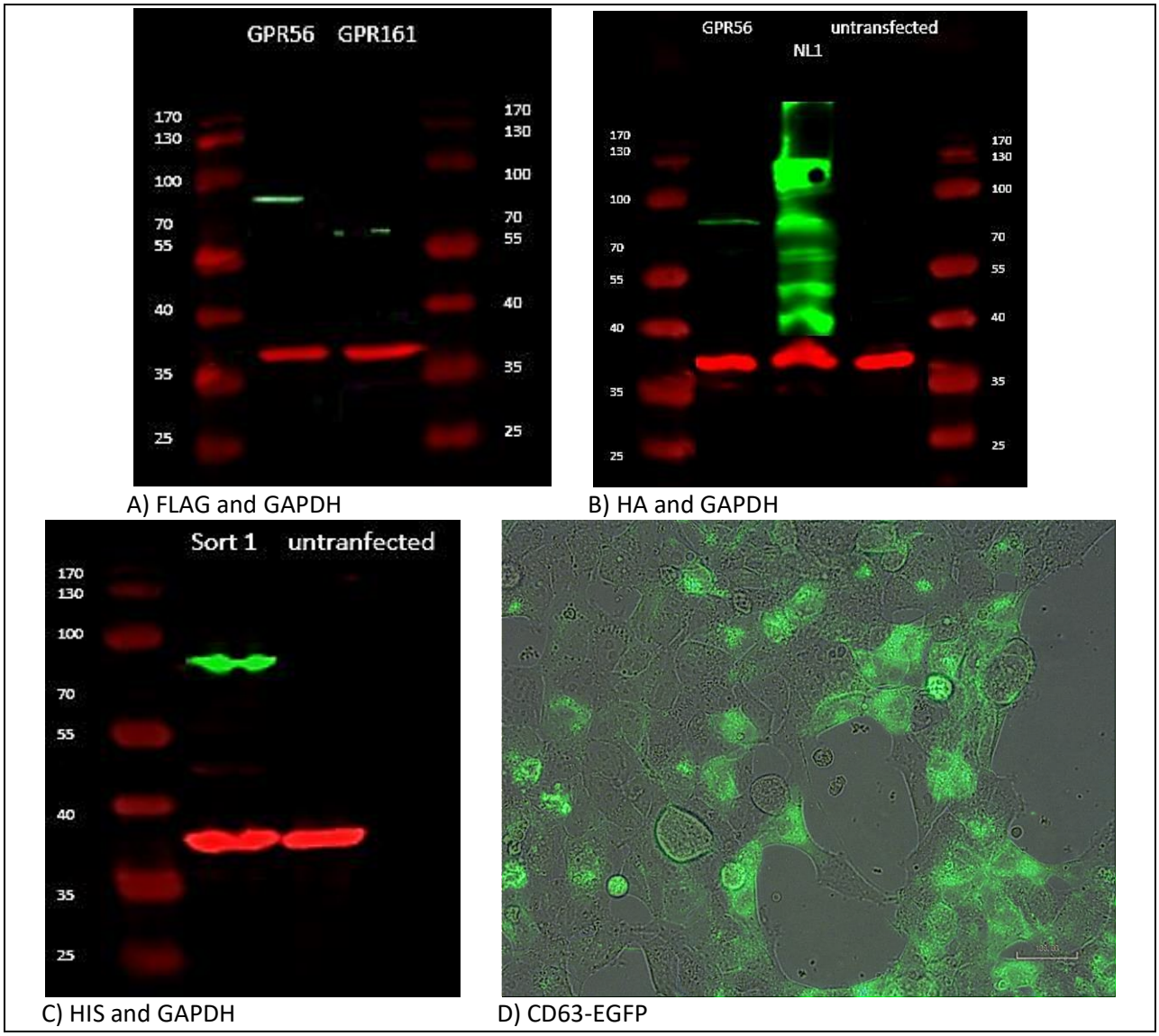

Figure 12: Proven Methods for analysis of transfected HEK293T cells with Receptor candidates

The western blots show the expression of GAPDH (red), as well as the FLAG-tag (A – green), HA-tag (B – tag) and HIS-tag (C – green) of the special receptors. GAPDH has a size of 37kDa and serves as loading control of all blots. A) GPR56 (77kDa) and GPR161 (60kDa) were detected by a FLAG antibody. B) GPR56 had a HA-tag in addition of the FLAG-tag. Also neuroligin 1 (NL1 - 93kDa) was detected by means of an HA antibody. C) Sortilin 1 (Sort 1 - 92kDa) was detected due to the HIS-tag. The markers on the left and right side provide information on the approximate size of the proteins sought from 25kDa to 170kDa. D) The receptor CD63 was visualized and detected using the EGFP-tag and fluorescence microscopy. Magnification: 100x; Scale: 100µm

3.2 Interaction of specific glycosaminoglycan's with viral proteins during the entry process

3.2.1 The role of free heparan sulfate for viral binding to the cell surface

Heparan sulfate is a highly negatively charged extracellular matrix polysaccharide and has a positive influence on viral heparan sulfate binding proteins, because the virus can reach the cell membrane for entry. Heparan sulfate on the cell membrane are bound with a proteoglycan molecule. For this reason, it´s important to know which main influence has the heparan sulfate proteoglycans for the viral entry of HERV-K (HML-2).

To obtain a precise overview of the task of cellular glycosaminoglycan´s various concentrations of free heparan sulfates were incubated with HEK293T cells and the viruses used. After incubation of heparan sulfate with the virus, the mixture was added to the cells and cultured. Due to the luciferase formation of the pseudotyped viruses, it was possible to measure entry into the cell. It turned out that increasing the concentration of heparan sulfate does not improve the entry of the virus, but worsens it. The lowest infection rate was reached at 400g/ml heparan sulfate, but it has no effect to the VSV-G. The infection was reduced from 100% to about 40% due to the heparan sulfate concentration. A slight increase in the infection rate of Δc1 of approximately 110% was achieved with the use of 50g/ml. The infection rate was normalized to the untreated cells and set to 100%. The functionless virus mutants of Δc1 and VSV-G, as well as the PBS control (mock), had no luciferase activity in the cells after infection.

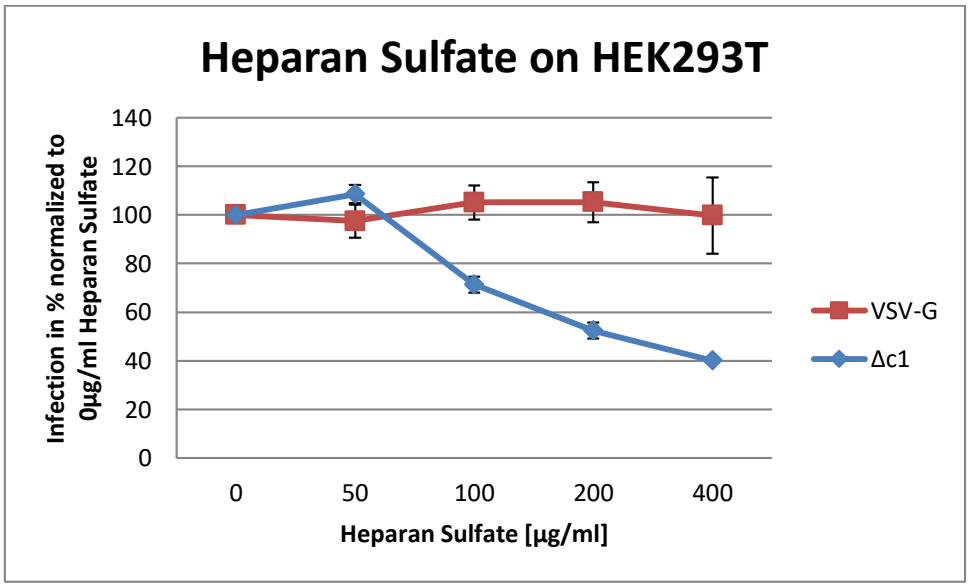

Figure 13: Infection rate after heparan sulfate incubation on HEK293T cells

The diagram shows the entry of the pseudotyped HI viruses Δc1 and VSV-G in HEK293T cells when incubated with 0-400g/ml heparan sulfate. The infection rate was measured by viral firefly luciferase activity and normalized to untreated cells and set to 100%. The non-functional virus mutants R140C and VSV-mutant, as well as the PBS control (mock), did not show luciferase activity after infection. Due to the biological replicates a standard deviation was determined.

3.2.2 Enzymatic digestion of heparan sulfate with heparinase I/III

Further evidence that heparan sulfates are important key players in the entry of HERV-K was the enzymatic digestion by heparinase I/III from the surface of SK-Mel28 cells. Heparinases belongs to the family of lyases, specifically those carbon-oxygen lyases acting on polysaccharides (Linhardt *et al.*, 1990). The cell line was cultured with three different concentrations of heparinase I/III (blend) and infected with pseudotyped viruses. The resulting luciferase activity was measured and show that the infection rate decreased with increasing heparinase activity. The infection with Δc1 could be reduced by up to 50%, whereby the VSV-G infection remained almost unaffected. The functionless virus mutants of Δc1 and VSV-G, as well as the PBS control (mock), had no luciferase activity in the cells after infection.

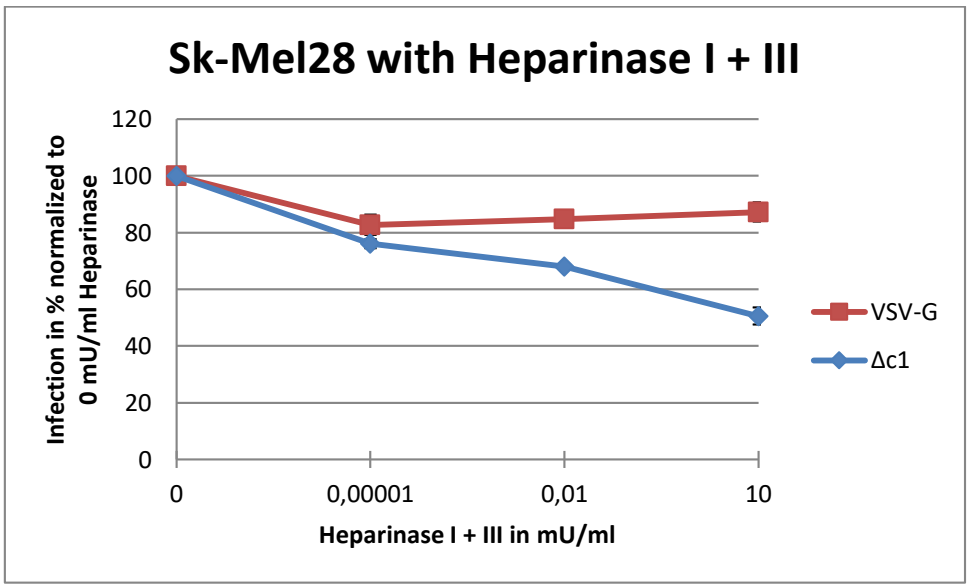

Figure 14: Infection rate after heparinase I/III digestion on Sk-Mel28 cells
The diagram shows the infection rate in % of Δc1 and VSV-G pseudotyped HIV. The viruses infected Sk-Mel28 cells after treatment of 0-10mU/ml heparinase I/III. The infection rate was measured by viral firefly luciferase activity and normalized to untreated cells and set to 100%. The non-functional virus mutants R140C and VSV-mutant, as well as the PBS control (mock), did not show luciferase activity after infection. Due to the biological replicates a standard deviation was determined.

3.2.3 Chemical inactivation of cell surface sulfation by sodium chlorate

Sodium chlorate inhibits the synthesis of the sulfate donor PAPS, thereby reducing cell surface sulfation. The first experiments were carried out by incubating the Sk-Mel28 cells for one hour with different concentrations of sodium chlorate. The diagram in figure 15 shows that sodium chlorate did not affect the infection of Δc1 and VSV-G pseudotyped HI viruses. It shows the luciferase activity of the infected viruses and was plotted logarithmically. It can be seen that the negative controls R140C, VSV-mut and mock had no luciferase activity, whereas VSV-G had a constant infectivity at all concentrations.

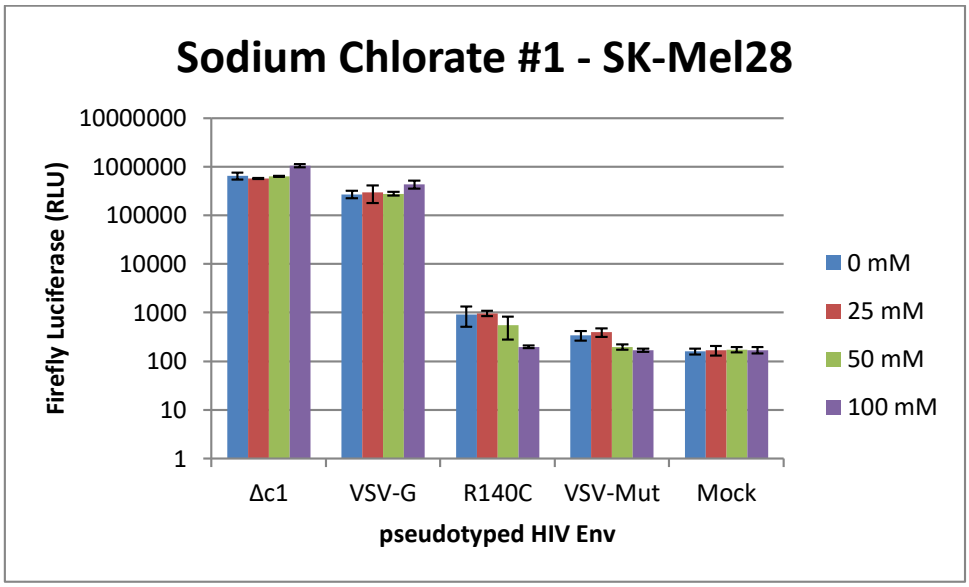

Figure 15: Viral firefly luciferase activity after incubation for 1h at 37°C with sodium chlorate
The cell line Sk-Mel28 was incubated for 1 hour at 37°C with 0-100mM sodium chlorate and then infected with pseudotyped HIV. The diagram shows the firefly luciferase activity after infection with Δc1, VSV-G, R140C and VSV-Mut, which was displayed logarithmically. The non-functional virus mutants R140C and VSV-mutant, as well as the PBS control (mock), did not show luciferase activity after infection. Due to the biological replicates a standard deviation was determined.

Due to the fact that the infection rate of Δc1 remained unchanged, the experimental setup was changed and the cell line cultured for two passages with three different concentrations of sodium chlorate. By this experimental change, the rate of infection of Δc1 could be reduced to 10%, whereas the infection with VSV-G remained unchanged at 100%. Thus, it can be said that with increasing sodium chlorate concentration, the infection rate of HERV-K decreased.

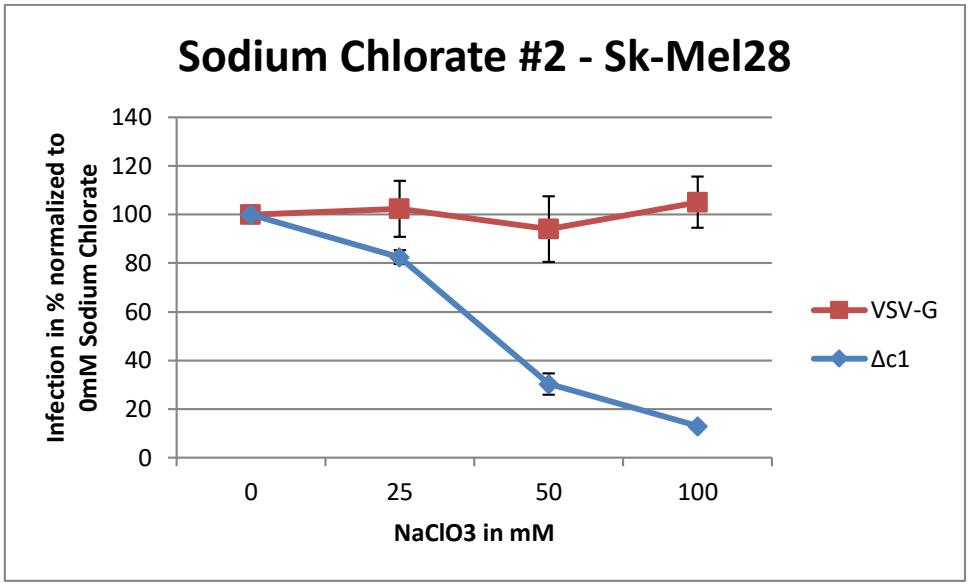

Figure 16: Viral firefly luciferase activity after incubation for 2 passages with sodium chlorate

The cell line Sk-Mel28 was incubated for 2 passages with 0-100mM sodium chlorate and then infected with pseudotyped HIV. The diagram shows the firefly luciferase activity after infection with Δc1 and VSV-G, which was normalized to untreated cells and set to 100%. The non-functional virus mutants R140C and VSV-mutant, as well as the PBS control (mock), did not show luciferase activity after infection. Due to the biological replicates a standard deviation was determined.

To verify the expression profile of heparan sulfates, various western blots were prepared. One antibody was used which generally detects heparan sulfates and another antibody detects syndecan-1. Syndecan-1 is a cell surface heparan sulfate proteoglycan and functions as an integral membrane protein, which is important for disease pathogenesis. On the one hand, the left blot shows that the GAPDH expression of the Sk-Mel28 cell line remained the same at 37kDa and thus the loading control was successful, as the same protein concentration was used for the blot. Based on the green bands at 32kDa syndecan-1 expression could be detected. It could be seen that syndecan-1 concentration decreased with increasing sodium chlorate concentration. In the right blot, an antibody was used for all heparan sulfates in general. Here, at 32kDa the decreasing syndecan-1 expression was best seen by the green bars, whereas the GAPDH concentration (red bars at 37kDa) remained the same. The cell line Colo205 should server as a positive control, as they contain a high amount of syndecan-1 (figure 22B). Due to the low yield of GAPDH, however, it is difficult to draw a connection to syndecan-1 expression.

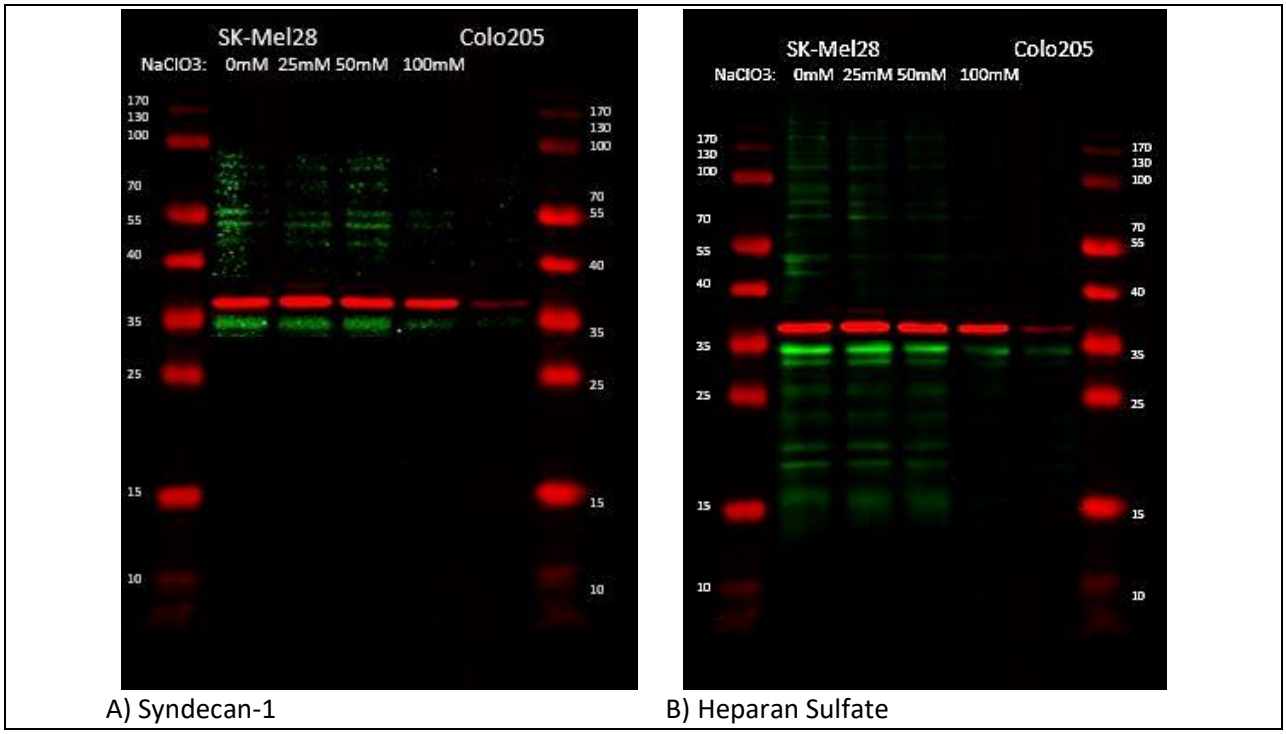

A) Syndecan-1 B) Heparan Sulfate

Figure 17: Western Blot analysis of HSPG´s after sodium chlorate cultivation

The left blot (A) shows the detection of GAPDH (red) at 37kDa and syndecan-1 (green) at 32kDa. The right blot (B) shows the expression of GAPDH (red) at 37kDa and various heparan sulfate proteoglycans (green). The HSPG Syndecan-1 at 32kDa on the right blot was particularly good to detect. For analysis, lysates of Sk-Mel28 cultured with different concentrations of sodium chlorate were used. Colo205 should serve as a positive control for syndecan-1. However, since the control GAPDH is only slightly visible, the detection of syndecan-1 is difficult. The markers on the left and right side provide information on the approximate size of the proteins sought from 10kDa to 170kDa.

Due to the microscopically recognizable changes in the proliferation rate of the cells due to the different concentrations of sodium chlorate, a growth curve was created. For this, the cells were cultured for 2 weeks with sodium chlorate and counted daily. After 2 days, the cells adapted to the environment and have gone into the exponential phase. The maximum cell division that occurred at this stage ended after about 9 days, after which the cells were in the plateau phase. In this section, the detaching cells and cells in mitosis phase are in equilibrium. After another 3 days in culture, the experiment was terminated.

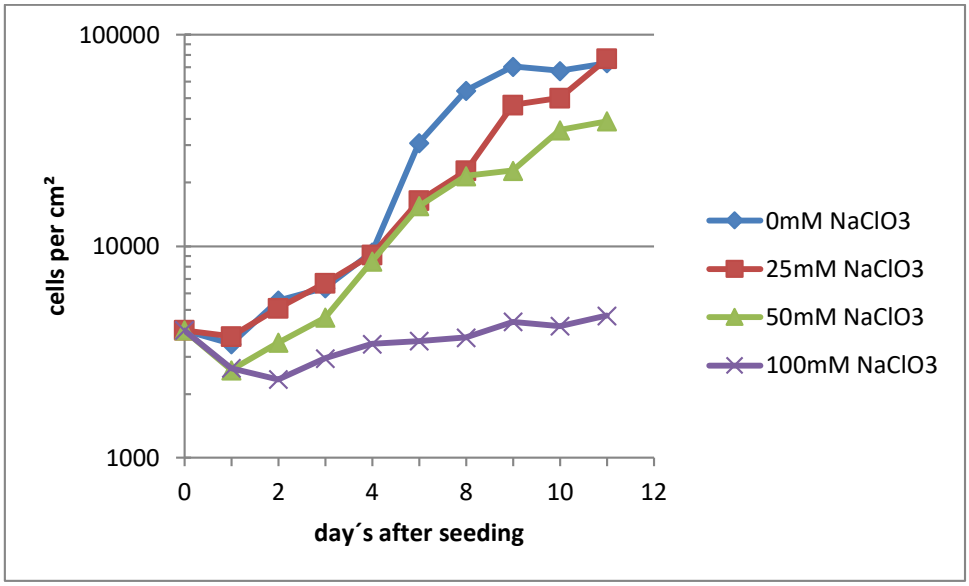

Figure 18: Growth Curve for Sk-Mel28 cultured with and without sodium chlorate
The cell line Sk-Mel28 was cultured in 6-well plates without, with 25mM, 50mM and 100mM sodium chlorate and a well counted daily. Every two days, a change of medium with fresh sodium chlorate was carried out. The cells per cm² were applied logarithmically.

In table 17 it can be seen that the population doubling time (PDT) of the Sk-Mel28 cell line with 100mM sodium chlorate is 5.5 times higher than that of the remaining cells. The cells without sodium chlorate had a PDT of 29 hours, with a culturing with 25mM a PDT of 34 hours and at 50mM sodium chlorate of 33.5 hours was determined. In contrast, culturing with 100mM indicated that the PDT increased to 166 hours.

TABLE 16: Population doubling time of Sk-Mel28 after sodium chlorate cultivation

Conditions	PDT in hours
Sk-Mel28 with 0 mM $NaClO_3$	29.1
Sk-Mel28 with 25 mM $NaClO_3$	34.3
Sk-Mel28 with 50 mM $NaClO_3$	33.5
Sk-Mel28 with 100 mM $NaClO_3$	166.4

3.2.4 Overexpression of syndecan-1 on the cell surface of HEK293T

To evaluate that syndecan-1 is an important factor for HERV-K entry, several cell lines were overexpressed with this protein. For this, E. coli were transformed with the SDC1 plasmid and selected with ampicillin. After the reproduction of the cells and isolation of the plasmids by the Quiagen Maxi Kit, the plasmid was cut with NotI and visualized by using gel electrophoresis and ethidium bromide. The gel pattern showed the expected sizes after digestion (+) at around 4700 and 2500 base pairs and thus could be used for further experiments.

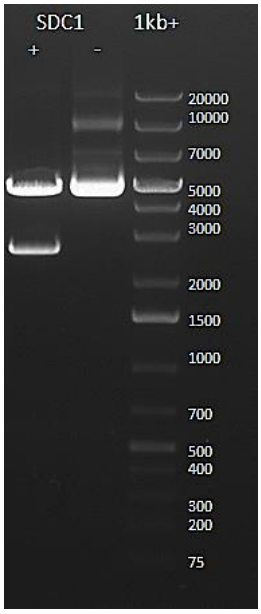

Figure 19: Gel electrophoresis after enzymatic digestion of syndecan-1 plasmid

The plasmid SDC1 was digested by the enzyme NotI for one hour at 37°C and applied to the gel (+). The control was the undigested plasmid, which is marked with (-). The gel was running for 1 hour at 90V and the marker on the right side shows the size of the bands from 75 to 20,000 bases.

After infection with HERV-K pseudotyped HIV and various control viruses, the luciferase activity was measured and evaluated in the following diagram. Due to the luciferase formation of the pseudotyped viruses, it is possible to measure entry into the cell. The diagrams in the figures 20 and 21 shows that a syndecan-1 overexpression did not affect the infection of Δc1 and VSV-G pseudotyped HIV. The cell line HCT116 was used because the cells express no syndecan-1 (figure 22B) and the entry of Δc1 is difficult. However, expression of syndecan-1 in HCT116 did not result in increased Δc1 entry into the cell. The diagrams show the luciferase activity of the infected viruses and was plotted logarithmically. It can be seen that the negative controls R140C, VSV-Mut and mock had no luciferase activity, whereas VSV-G had a constant infectivity.

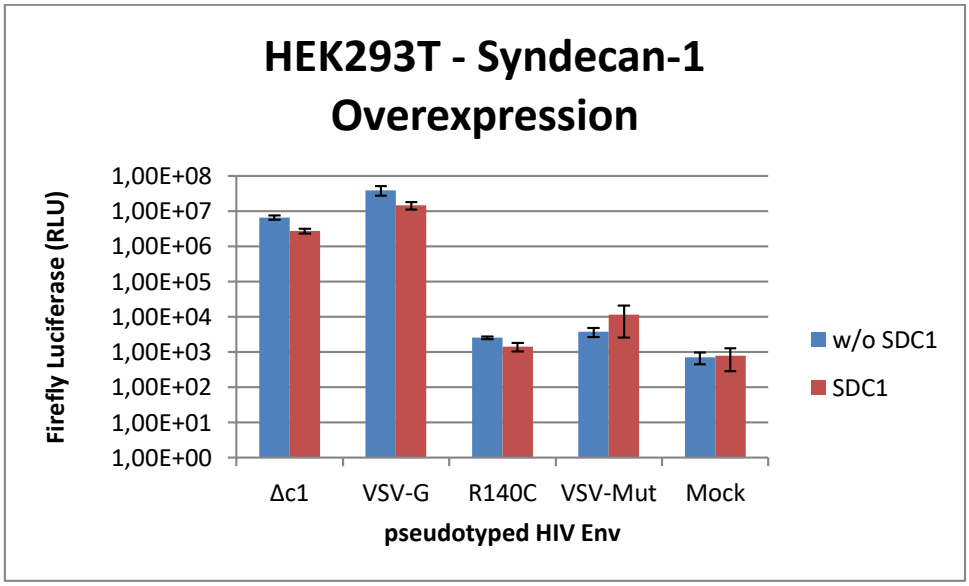

Figure 20: Viral infection of syndecan-1 overexpressed HEK293T cells

The cell line HEK293T was transfected with syndecan-1 and then infected with pseudotyped HIV. The diagram shows the firefly luciferase activity after infection with Δc1, VSV-G, R140C and VSV-Mut, which was displayed logarithmically. The non-functional virus mutants R140C and VSV-mutant, as well as the PBS control (mock), did not show luciferase activity after infection. Due to the biological replicates a standard deviation was determined.

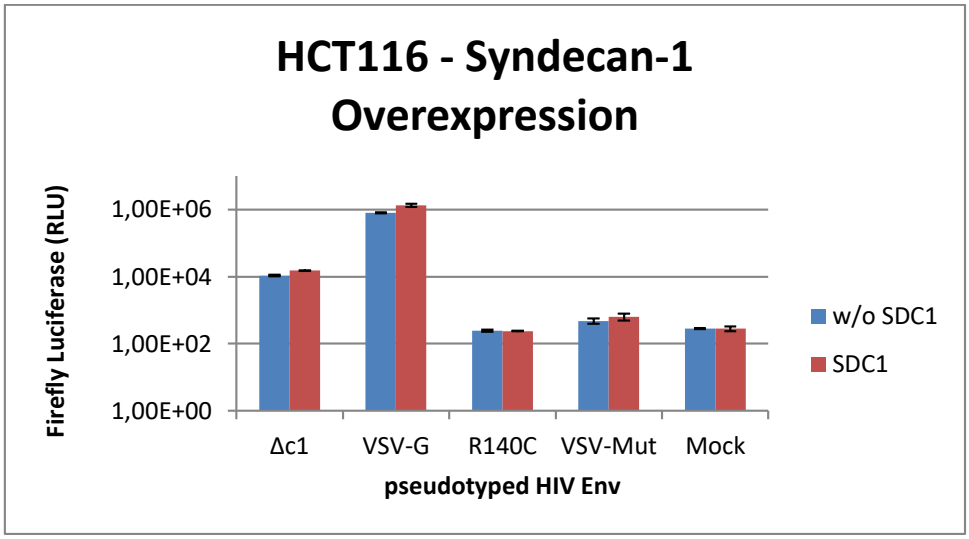

Figure 21: Viral infection of syndecan-1 overexpressed HCT116 cells

The cell line HCT116 was transfected with syndecan-1 and then infected with pseudotyped HIV. The diagram shows the firefly luciferase activity after infection with Δc1, VSV-G, R140C and VSV-Mut, which was displayed logarithmically. The non-functional virus mutants R140C and VSV-mutant, as well as the PBS control (mock), did not show luciferase activity after infection. Due to the biological replicates a standard deviation was determined.

To assess a successful transfection with syndecan-1, a western blot (figure 22A) with the prepared cell lysates was performed. The specific antibody for syndecan-1 detected the syndecan-1 core at 77kDa (green) for both transfected cell lines. GAPDH (red) was detected in all samples with equal intensity at 37kDa. To compare the transcript intensity, z-scores for the cell lines Colo205 and HCT116 of HSPG2 and syndecan-1 were determined (figure 22B). Based on these data, HCT116 was used for this experiment.

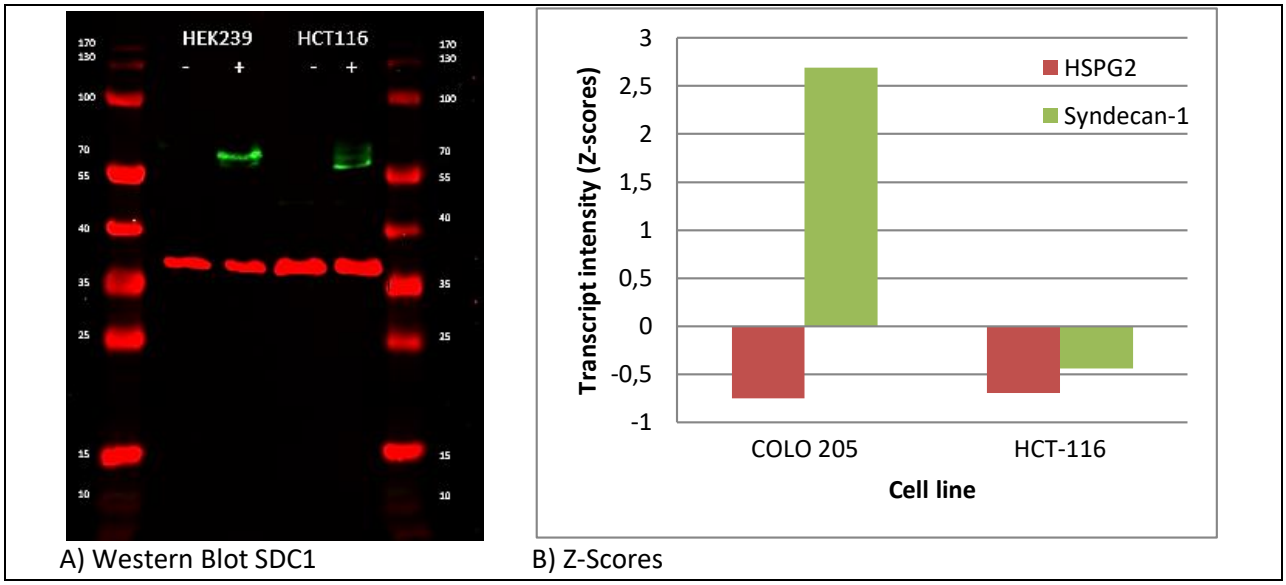

A) Western Blot SDC1 B) Z-Scores

Figure 22: Western Blot analysis of syndecan-1 transfected cells and specific Z-scores

A) The blot shows the detection of GAPDH (red) at 37kDa and the core of syndecan-1 (green) at 77kDa. For analysis, lysates of transfected HEK293T and HCT116 were used. The markers on the left and right side provide information on the approximate size of the proteins sought from 10kDa to 170kDa. B) The diagram shows the transcript intensity of Colo205 and HCT of HSPG2 (Perlecan) and syndecan-1. The values were determined by CellMiner NCI-60 Analysis Tool.

3.2.5 Reduction of syndecan-1 expression by specific shRNA´s

In order to analyze how the infection rate of pseudotyped HIV changes when the expression of syndecan-1 is reduced, the cells were incubated with special shRNA´s. A short hairpin RNA is an artificial RNA molecule with a tight hairpin turn. The expression of shRNA in the cell lines was done by the transfection of specific plasmids. It has the advantage, that this have a relatively low rate of degradation and turnover. In addition to the shRNA, the genetic information for puromycin resistance is also on the plasmid. Due to this fact, the successfully infected cells could be selected by puromycin. For a precise concentration, different values of 0-5µg/ml puromycin were added to untransfected Sk-Mel28 and HEK293T and cultured for several days. In figure 23 it could be seen that all HEK293T cells died at 1.5µg/ml and all Sk-Mel28 at 1µg/ml. For this reason, the transfected cells were cultured with these puromycin concentrations to obtain a stable transfected cell line.

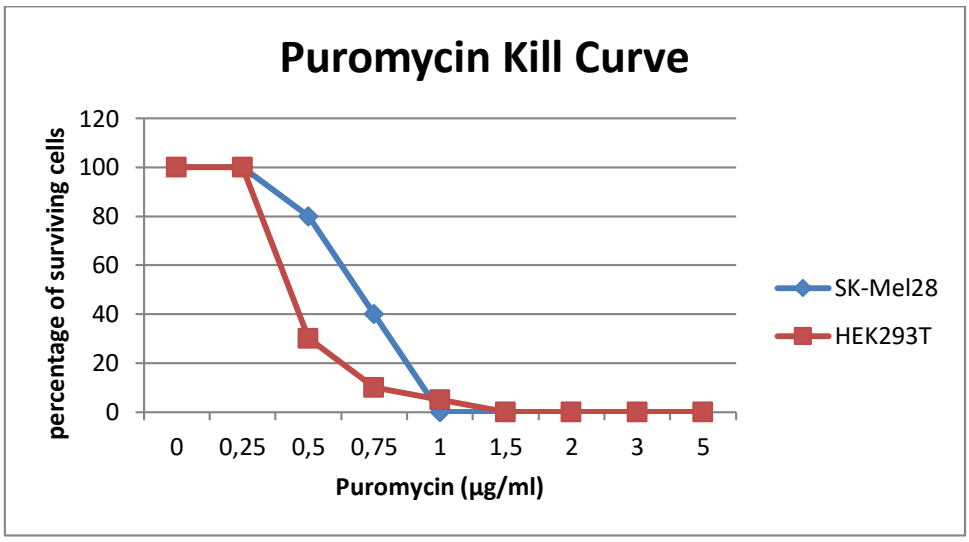

Figure 23: Puromycin kill curve for Sk-Mel28 and HEK293T
The diagram shows the minimal puromycin concentration at which untransfected HEK293T and Sk-Mel cells were no longer viable. Vitality was expressed in percentage of surviving cells. At 0.5µg/ml, a reduction in cell vitality was already evident. Cell death from Sk-Mel28 could be detected at 1µg/ml and from HEK293T at 1.5µg/ml.

After infection with HERV-K pseudotyped HIV and various control viruses, the luciferase activity was measured and evaluated in the following diagram. Due to the luciferase formation of the pseudotyped viruses, it is possible to measure entry into the cell. The diagram in figure 24 shows that a syndecan-1 reduction effect the infection rate of Δc1 pseudotyped HIV. It was used for the infection 1µg and 2µg of plasmids because prior the experiment, it was not clear which would be the optimal concentration for shRNA production. After evaluation of luciferase activity, it could be seen that a transfection of 2µg plasmid allowed a greater reduction of the Δc1 infection.

The entry of HERV-K could be reduced by 70% in HEK293T and by 40% in Sk-Mel28. The infection rate was normalized to the untreated cells and set to 100%. The functionless virus mutants of Δc1 and VSV-G, as well as the PBS control (mock), had no luciferase activity in the cells after infection.

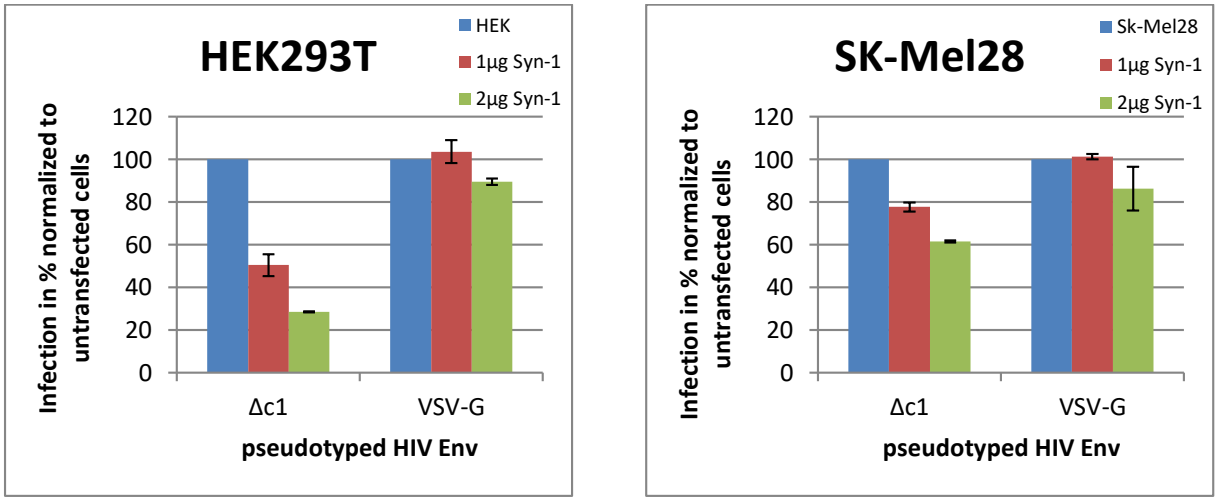

Figure 24: Viral infection of HEK293T and Sk-Mel28 after syndecan-1 reduction by shRNA
The cell line HEK293T (left) and Sk-Mel28 (right) was transfected with syndecan-1 shRNA (by a plasmid) and then infected with pseudotyped HIV. The diagram shows the firefly luciferase activity after infection with Δc1 and VSV-G, which was normalized to untreated cells and set to 100%. The non-functional virus mutants R140C and VSV-mutant, as well as the PBS control (mock), did not show luciferase activity after infection. Due to the biological replicates a standard deviation was determined.

To verify the expression profile of syndecan-1 in shRNA transfected Sk-Mel28 cells, a western blot was performed with a specific syndecan-1 antibody. For this experiment the cell lysates from no transfected and with 1µg and 2µg plasmid transfected cells were used. The blot shows that the GAPDH expression of the Sk-Mel28 cell line remained the same in every sample at 37kDa. Based on the green bands at 32kDa syndecan-1 expression could be detected. It could be slightly seen that after transfection the syndecan-1 concentration decreased with increasing shRNA plasmid concentration. In HEK293T cells it was not possible to detect syndecan-1 by western blot.

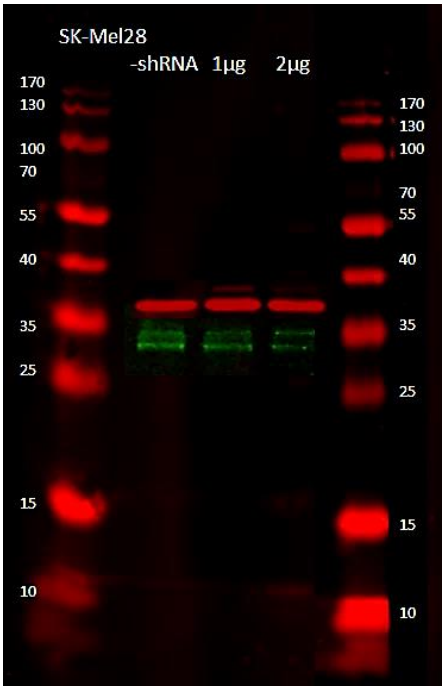

Figure 25: Western Blot analysis of syndecan-1 shRNA transfected Sk-Mel28 cells

The Blot shows the expression of GAPDH (red) and syndecan-1 (green) of shRNA transfected Sk-Mel28 cells. The shRNA inhibits the mRNA of syndecan-1 and thus prevents protein expression. The markers on the left and right side provide information on the approximate size of the proteins sought from 10kdA to 170kDa. The samples from left to right are untransfected cells and then transfected cells with 1µg and 2µg shRNA plasmids. No syndecan-1 could be detected in HEK293T cells. For this reason, the blot was not shown.

4. Discussion

4.1 The importance of specific receptors for the entry of HERV-K (HML-2) into the cell

The human genome consists of 8% retroviral elements with terminal LTRs, 4.7% of which are human endogenous retroviruses (HERVs) (Bannert and Kurth, 2004; Beimforde *et al.*, 2008; Lander *et al.*, 2001). HERVs were also once exogenous retroviruses that infected human endocrine cells, endogenized and multiply integrated into the genome by reinfection and retrotransposition (Gifford and Tristem, 2003). The replication of retroviruses begins by infection of the host cell. The virus, mediated by its glycosylated cot proteins, attaches to specific receptors of the cell. It leads to the fusion of the virus envelope with the plasma membrane or to the endocytosis of the entire viral particle. For this reason, one of the two main tasks in this work was to find the specific receptor for HERV-K entry into the cell. For this purpose, the receptors of the syncytins and various other receptor candidates were considered, which were analyzed in many previous work in the working group.

The env genes of HERV-W and HERV-FRD, better known as syncytin-1 and syncytin-2, influence placental development (Bannert *et al.*, 2018). The human syncytin-1 is a cell-cell fusion protein and is involved in the fusion of the cytotrophoplasts cells and thus leads to the formation of the polynuclear syncytiotrophoblast (Blond *et al.*, 1999; Blond *et al.*, 2000; Mi *et al.*, 2000; Pötgens *et al.*, 2004). The syncytin-1 receptor is the sodium dependent amino acid transporter 1 (ASCT1 or SLC1A4) and 2 (ASCT2 or SLC1A5). Syncytin-2 carries through its immunosuppressive properties of mother-to-child tolerance during pregnancy (Malassiné *et al.*, 2007). The syncytin-2 receptor is the sodium-dependent lysphosphatidylcholin symporter 1 (MFSD2A), which plays an essential role for blood-brain barrier formation and function and acts as a receptor in placenta. Recent studies have pointed to the expression of the HERV-K envelope protein in cells of the placental cytotrophoblast, but not in the syncytiotrophoblast. Therefore, it can be assumed that syncytin receptors also play a significant role in the entry of HERV-K.

For this experiment, the cell line HEK293T was transfected with the receptors ASCT1, ASCT2 and MFSD2A. Already a microscopic control of the cells after 24 hours showed that the cells started to clump together after transfection. Due to the property of cell-cell fusion, which can be seen in figure 8, one can assume that the transfection was successful. The western blot also showed a successful transfection efficiency, since the Flag-tag of the transfected receptors could be detected in all samples, except of the untransfected cells. Due to this fact, the infection experiments could be carried out. For this purpose, pseudotyped HIV were produced and infected with a syncytin-1 and syncytin-2 envelope. The results of

the firefly luciferase assay showed that transfection of the specific receptors resulted in increased syncytin-1/2 virus entry into the cells. This and the consistent infection rate of VSV-G indicates that infection with HERV-K pseudotyped HIV (Δc1) can be successfully evaluated. The viral entry experiments with Δc1 did not result in a higher infection rate after transfection of syncytin receptors. This was due to the fact that none of the samples had a higher infection than untransfected HEK293T cells. Due to this fact, it could be assumed that the receptors ASCT1, ASCT2 and MFSD2A were not the specific receptors for the entry of HERV-K (HML-2).

This was the reason that new receptor candidates had to be used for further entry experiments. Previous work by N. Bannert and A. Richter compared different gene profiles of successfully infected cells with HERV-K and thus identified potential receptors that might be specifically involved in the onset of the virus. These receptors were the G protein-coupled receptors 56 and 161, the cell surface receptor CD63, the neural cell adhesion molecule L1CAM, the Golgi sorting receptor sortilin-1, and the cell surface protein neuroligin-1. The plasmids of these receptors were brought into the cells by means of PEI transfection and checked for successful expression by western blot and fluorescence. The images in figure 12 showed that GPR56, GPR161, Sort1 and CD63 could be successfully detected. Due to the non-specific bands in Neuroligin-1 and the fact that L1CAM and BC-GPR56 (another plasmid for GPR56) had no protein tag, expression could not be detected here. The infection experiments with the pseudotyped HIV showed that VSV-G had a consistent infection in all samples. Slight differences compared to the untransfected cells were seen in the infection with Δc1. However, especially transfection with GPR56 increased the infection rate 3-fold to the untransfected cells. This suggests that GPR56 may play an essential role in the specific entry of HERV-K. The adhesion G protein-coupled receptor G1 (GPR56) is involved in cell adhesion and probably in cell-cell interactions. Collagen III is a ligand of GPR56 in the developing brain and the receptor binds transglutaminase 2 (TG2) to suppress tumor metastasis (Luo *et al*., 2012).

4.2 Heparan sulfate proteoglycans on the cell surface as the main component for the adhesion of HERV-K (HML-2)

HSPG´s are a group of proteins that have at least one covalently linked heparan sulfate (HS) side chain. This side chains bind a variety of growth factors, extracellular matrix factors and other proteins, indicating that HS side chains bind to cell adhesion or regulation of cell division activity (Carey, 1997). In addition, it is known that various pathogens interact with the heparan sulfate proteoglycans, because the HS has a positive influence on viral heparan sulfate binding proteins. Often, binding of a viral protein to heparan sulfate is only the first step in a cascade of interactions between virus and cell that is

required for viral entry into the cell and the initiation of infection. As many microorganisms, HIV-1 also interacts with heparan sulfates, because the gp120 protein which is important for the first contact with the CD4 receptor, interacts with a variety of HS (Connell and Lortat-Jacob, 2013). Zhang *et al.* described in their paper that the Coxsackievirus A16 uses surface HSPGs as a binding receptor. Coxsackievirus A16 (CVA16) is one of the major pathogens responsible for hand, foot and mouth disease, which affects more than two million children in the Asian-Pacific region annually (Zhang *et al.*, 2017). This and many other experiments were the motivation to analyze the role of heparan sulfate proteoglycans in the entry of human endogenous retroviruses into the cell.

One of the main experiments was the interaction of free heparan sulfate with the cell surface and the viruses used for the infection. The diagram in the figure 13 showed that the infection rate of Δc1 decreased with increasing heparan sulfate concentration. The reduction of the infection down to 40% could be due to the fact that the HS-binding proteins on the virus surface was saturated with free heparan sulfate and thus the virus no longer had the possibility to bind to the cell surface. The HS-binding proteins are normally responsible for allowing the virus to reach and adhere the cell. However, this became impossible with increasing concentration of free HS. Furthermore, it is possible that heparan sulfate interacts with the potential receptor GPR56 because not only collagen III and TG2, but also heparin and heparan sulfate interact with the adhesion protein. Hence, it is possible that heparin and heparan sulfate act as a suppressor (antagonist) of GPR56 receptor function, in part, by inhibiting GPR56 receptor shedding, thereby trapping and masking the tethered Stachel peptide agonist and preventing the activation of the signaling pathways (Chiang *et al.*, 2016). These two facts could be responsible for the reduction of the infection rate. In many papers, heparan sulfate is described as an attachment factor for a wide variety of viruses. Zhang *et al.* used in his work soluble heparin to investigate the role of heparan sulfate-specific glycosaminoglycan's in CVA16 infections. Heparan sulfate is structurally related to heparin, only it has less N- and O-sulfate residues and more N-acetyl groups. They found, that concentrations of more than 1.56mg/ml heparin could inhibit the cellular attachment of CVA16.

An enzymatic digestion of heparan sulfate with heparinase I and III also reduced the infection rate of HERV-K (HML-2) by up to 50%. Heparinases belongs to the family of lyases, specifically those carbon-oxygen lyases acting on polysaccharides. The enzyme cleaves the glycosidic linkage between hexosamines and uronic acids and are known to cleave heparan sulfates selectively, via an elimination mechanism. Heparinase I cleaves highly sulfated heparan sulfate chains and heparinase III less sulfated chains. In combination the enzyme can produce a near complete depolymerization of polysaccharide chains to disaccharides (Linhardt *et al.*, 1990). The enzymatic digestion with a maximum of 10mU/ml heparinase I/III ensured that the HS side chains were detached from the proteoglycans and thus were no

longer present. Because of this, HERV-K was unable to bind to the cell surface and infect the cells at full rate. Plochmann *et al.* showed that heparan sulfate is an attachment factor for foamy viruses. Enzymatic digestion of heparan sulfate on HT1080 cells diminished permissivity for prototype foamy virus entry by a factor of at least 500 (Plochmann *et al.*, 2012). Nasimuzzaman and Persons showed that concentrations of 4mU/ml heparinase III in NIH3T3 cells could reduce the infection rate of FV up to 10%. The analysis was not carried out as in the experiments described here by means of luciferase, but a formed GFP signal after successful infection was determined by means of FACS analyzes (Nasimuzzaman and Persons, 2012).

Not only the enzymatic digestion but also the chemical inactivation of cell surface led to the reduction of the HERV-K infection rate. Sodium chlorate inhibits the synthesis of the sulfate donor PAPS, thereby reducing cell surface sulfation. The sulfation is the major biosynthetic modification of glycosaminoglycan's and the unique and complex sulfation patterns enable them to bind specifically to many biomolecules and regulate diverse biological processes (Funderburgh, 2000; Mikami and Kitagawa, 2013; Perrimon and Bernfield, 2000). After incubation with sodium chlorate for 1 hour at 37°C did not give the expected result, the experiment was repeated after the cells were cultured for several days with sodium chlorate. The diagram in figure 16 shows that a high sodium chlorate concentration reduces the infection rate of HERV-K. A concentration of 100mM reduced the infection by up to 90% compared to 0mM sodium chlorate. However, at this concentration, a microscopic change in cell morphology was evident, producing a growth curve. The growth curve in figure 18 shows strong proliferation changes of the Sk-Mel28 cell line with 100mM sodium chlorate. Here, the population doubling time increased by 5.5-fold compared to 0mM, 25mM and 50mM sodium chlorate. Based on this fact, it can be said that the maximum concentration of sodium chlorate to be used was 50mM and thus the infection rate of HERV-K could be reduced to 30%. This is the evidence that the sulfation pattern of the glycosaminoglycan's on the cell surface is important for the attachment of the virus. The reduction in sulfation was detected by western blot analysis and confirms the statement that an increasing concentration of sodium chlorate the sulfation and thus the infection rate decreased. Sodium chlorate inhibited the sulfation of HS and thus eliminated the epitope recognized by the antibody. Therefore, sodium chlorate-treated cells showed reduction in HS expression compared with untreated control cells. Also in the paper by Nasimuzzaman and Persons, sodium chlorate was used to prevent the sulfation of HS. It was found, that even a concentration of 25mM reduced the entry of FV in A549 cells by up to 95%.

Another experiment was a HERV-K infection with overexpressed syndecan-1 in HEK293T and HCT116 cells. Syndecan-1 is a transmembrane (type I) heparan sulfate proteoglycan and is a member of the syndecan family. The syndecans mediate cell binding, cell signaling and cytoskeletal organization and

syndecan receptors are required for internalization of the HIV-1 tat protein (Zhou *et al.*, 2008). The syndecan-1 protein functions as an integral membrane protein and participates in cell proliferation, cell migration and cell-matrix interactions via its receptor for extracellular matrix proteins. After transfection with the specific plasmids for syndecan-1 expression, the cells were infected with various pseudotyped HIV. The detection of firefly luciferase in the cells showed that despite overexpression of syndecan-1, an increased HERV-K entry into HEK293T cells did not occur. Also in HCT116 cells, which have only a low infection rate with HERV-K, an overexpression could not achieve the expected success. Thus, it can be said that a greater amount of syndecan-1 proteins on the cell surface did not result in an increased HERV-K entry in the cells. To check the transfection efficiency syndecan-1 was detected by western blot. It could be seen that after transfection the proteins in the cells were increasingly expressed, since the core protein is recognizable at 77kDa.

Since an overexpression of syndecan-1 did not result in increased HERV-K entry into the cells, the expression was reduced by specific shRNAs. A short hairpin RNA is an artificial RNA molecule with a tight hairpin turn. The expression of shRNA in the cell lines was done by the transfection of specific plasmids. The reduction of syndecan-1 by transfection of 1µg and 2µg plasmid in HEK293T and Sk-Mel28 cells reduced the infection rate of HERV-K. In HEK293T the infection could be reduced up to 30% with 2µg plasmid. This suggests that the HS-binding protein of the virus had only a small ability to adhere to the cells and penetrate. The detection of syndecan-1 by western blot showed that expression decreased with increasing plasmid transfection. Therefore, it could be assumed that the reduction in the infection rate was due to the inhibition of syndecan-1 expression. Shi *et al.* described that syndecan-1 is an important receptor for the attachment of hepatitis C virus to the cell surface of hepatocytes. Hepatitis C virus (HCV) is a common cause of chronic liver diseases such as hepatitis, cirrhosis, and liver cancer. It is an enveloped RNA virus containing a single positive-sense RNA genome that encodes a polyprotein precursor of 3,000 amino acids (Choo *et al.,* 1989). The knockdown of SDC1 expression by small interfering RNA (siRNA)-induced gene silence resulted in a significant reduction of HCV attachment to Huh-7.5 cells and stem cell-differentiated human hepatocytes (Shi *et al.*, 2013).

Nasimuzzaman and Persons described in their work that syndecan-1 has an important role in the infection with the foamy virus. Raji cells, which lack HS and were largely resistant to FV, were rendered more permissive through ectopic expression of syndecan-1, which contains HS. In contrast, mutant syndecan-1-expressing cells were largely resistant to FV. There findings indicate that cellular HS is a receptor for FV. Also two mutant CHO cell lines lacking cell surface HS were largely resistant to FV attachment and transduction. They described in their study, that they have found that cell membrane-associated HS serves as a receptor for FV based on the following evidence: (i) HS-deficient cells are less permissive to FV whereas wild-type cells are permissive, (ii) enzymatic removal of HS or chemical

removal of the sulfate group from cells greatly reduces FV permissiveness, and (iii) induction of HS expression makes cells more permissive to FV (Nasimuzzaman and Persons, 2012). This was also demonstrated in these carried experiments for HERV-K entry. Only the expression of syndecan-1 in different cells could not increase the infection.

The research article „Reconstruction of the cell entry pathway of an extinct virus" was published in august 2018 and described a few parts from the experiments in this thesis. They published this paper during my work and confirmed the results of the viral entry of HERV-K (HML-2) in connection with the use of free heparan sulfate and the chemical inactivation of the cell sulfation. The major conclusion of this study was that heparan sulfate is a direct HERV-K attachment factor. They create a model (figure 26) for the entry of HERV-K, in which is shown the viral binding to heparan sulfate, the endocytosis in a dynamin-dependent, clathrin independent manner and an acidification of the endosome which is leading to membrane fusion and infection.

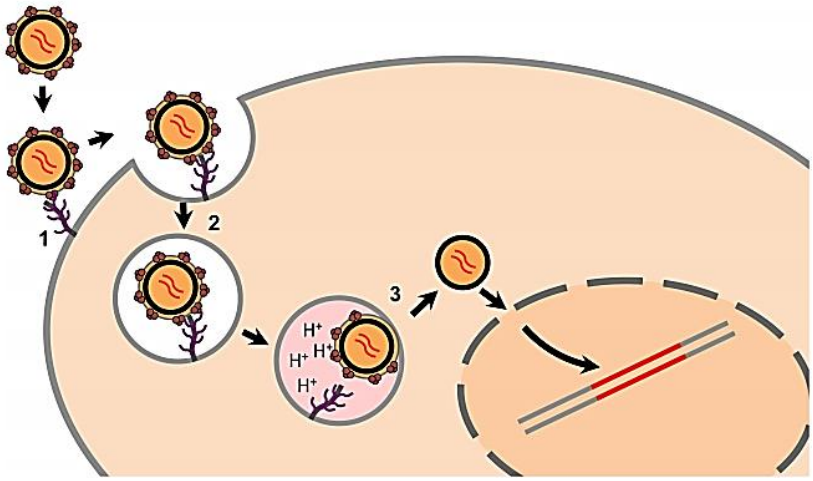

Figure 26: Model of HERV-K entry
1. HERV-K binds to HSPGs on the cell surface. 2. Endocytosis in a dynamin-dependent and clathrin-independent manner. 3. Releasing of the viral core into the cytoplasm by acidification of the endosome (Robinson-McCarthy *et al.,* 2018).

In contrast to this work, the experiments in this thesis showed that syndecan-1 in particular has an important role in viral attachment. Furthermore, it could be shown that not only the HSPGs can be responsible for the viral entry, since it was not possible to reduce the infection rate of HERV-K to zero by reducing the heparan sulfates. The receptor experiments proved that the G protein-coupled receptor 56 may be a specific factor for HERV-K entry. Thus, it could be said that the heparan sulfates such as syndecan-1 are responsible for attachment to the cells and GPR56 for endocytosis. To be able to make a 100% statement about this, further experiments should follow.

4.3 Outlook

In this work, it has been possible to show that heparan sulfate proteoglycans have an important role in the onset of HERV-K (HML-2). To further investigate the interaction between heparan sulfate and virus, it has been demonstrated that the heparan sulfate binding proteins on the viral envelope are responsible for contact with the cell surface. For example, binding experiments using surface plasmon resonance (SPR) analyzes could be performed. Here, heparan sulfates are coated on the specific prism and the virus is added after certain analytic steps. Based in the analysis of the date, it could be seen whether HERV-K binds specifically to the heparan sulfates. You could also use special heparan sulfates such as syndecan-1 and syndecan-2. As already shown, syndecan-1 is essential at viral entry because reduction of syndecan-1 molecules on the cell surface resulted in a reduction in the rate of infection. However, it is still important to see how the surface profile of the cells is built up. A pure western blot analysis is not enough, because you cannot be sure of the protein has reached its true destination. It is indistinguishable whether the receptor is on the cell surface or in the cytoplasm. For this reason, further work on this topic should explore the cell surface by using FACS analysis. It can be seen exactly whether the use of the shRNA for syndecan-1 could change the surface concentration. Furthermore, it can be seen whether overexpression with syndecan-1 led to the desired success on the surface of the cells. As can be seen in the western blot, the core protein of syndecan-1 was detected at 77kDa only in transfection with the specific plasmid. In contrast, the naturally occurring syndecan-1 became visible in Sk-Mel28 at a size of 32kDa. In order to determine the cause, FACS analyzes are essential.

In order to establish a connection between the G protein-coupled receptor 56 and the heparan sulfate proteoglycans, it is particularly important to see whether both proteins interact with each other. For this purpose, one can analyze whether heparan sulfate actually acts as an antagonist for the receptor and inhibits the signal cascade. In this case, it is necessary to know which reactions an activation of the receptor is triggered intracellularly and can follow. Only then can one determine and check exact interactions. However, this information should be easily ascertainable through special reading. In a potential interaction of HS with the GPR56, one could still draw conclusions about an interaction with HEERV-K. One approach would be to reduce the receptor expression via shRNA or to block certain signaling pathways within the cell. This allows one to see if the receptor is responsible for the entry of HERV-K (HML-2).

To analyze which of the different receptors is responsible for the entry of HERV-K should have the highest priority, as this could be essential for a possible drug development. At the present time, however, it can be said that various heparan sulfates and GPR56 could play a crucial role in the entry of HERV-K (HML-2). This should be one of the main theses for future work on this topic.

5. References

Alkhatib, G., Berger, E.A., 2007. HIV coreceptors: From discovery and designation to new paradigms and promise. European journal of medical research 12 (9), 375–384.

Aloia, R.C., Tian, H., Jensen, F.C., 1993. Lipid composition and fluidity of the human immunodeficiency virus envelope and host cell plasma membranes. Proceedings of the National Academy of Sciences of the United States of America 90 (11), 5181–5185.

Alves, C., Dourado, L., 2010. Endocrine and metabolic disorders in HTLV-1 infected patients. The Brazilian journal of infectious diseases : an official publication of the Brazilian Society of Infectious Diseases 14 (6), 613–620.

Anakok OF, 2016. Functional dissection of the HNRPA2B1-CBX3 ubiquitous chromatin opening element (A2UCOE). Thesis - King's College London, 22.

Andersson, M.L., Lindeskog, M., Medstrand, P., Westley, B., May, F., Blomberg, J., 1999. Diversity of human endogenous retrovirus class II-like sequences. The Journal of general virology 80 (Pt 1), 255–260.

Antony, J.M., Deslauriers, A.M., Bhat, R.K., Ellestad, K.K., Power, C., 2011. Human endogenous retroviruses and multiple sclerosis: Innocent bystanders or disease determinants? Biochimica et biophysica acta 1812 (2), 162–176.

Asundi, V.K., Carey, D.J., 1997. Phosphorylation of recombinant N-syndecan (syndecan 3) core protein. Biochemical and biophysical research communications 240 (2), 502–506.

Balada, E., Vilardell-Tarrés, M., Ordi-Ros, J., 2010. Implication of human endogenous retroviruses in the development of autoimmune diseases. International reviews of immunology 29 (4), 351–370.

Baltimore D., 1975. Tumor viruses: 1974 (39), 1187–1200.

Bannert, N., Hofmann, H., Block, A., Hohn, O., 2018. HERVs New Role in Cancer: From Accused Perpetrators to Cheerful Protectors. Frontiers in microbiology 9, 178.

Bannert, N., Kurth, R., 2004. Retroelements and the human genome: New perspectives on an old relation. Proceedings of the National Academy of Sciences of the United States of America 101 Suppl 2, 14572–14579.

Bannert, N., Kurth, R., 2006. The evolutionary dynamics of human endogenous retroviral families. Annual review of genomics and human genetics 7, 149–173.

Barré-Sinoussi F., Chermann J C., Rey F., Nugeyre MT., Chamaret S., Gruest J., Dauget C., Axler-Blin C., Vezinét-Brun F., Rouzioux C., Rozenbaum W., Montagnier L., 1983. Isolation of a T-lymphotropic retrovirus form a patient at risk for AIDS. Science (220), 868–871.

Beimforde, N., Hanke, K., Ammar, I., Kurth, R., Bannert, N., 2008. Molecular cloning and functional characterization of the human endogenous retrovirus K113. Virology 371 (1), 216–225.

Bittner JJ., 1936. Some possible effects of nursing on the mammary gland tumour incidence in mice. Science (84), 162.

Blond, J.L., Besème, F., Duret, L., Bouton, O., Bedin, F., Perron, H., Mandrand, B., Mallet, F., 1999. Molecular characterization and placental expression of HERV-W, a new human endogenous retrovirus family. Journal of virology 73 (2), 1175–1185.

Blond, J.L., Lavillette, D., Cheynet, V., Bouton, O., Oriol, G., Chapel-Fernandes, S., Mandrand, B., Mallet, F., Cosset, F.L., 2000. An envelope glycoprotein of the human endogenous retrovirus HERV-W is expressed in the human placenta and fuses cells expressing the type D mammalian retrovirus receptor. Journal of virology 74 (7), 3321–3329.

Bock, M., Stoye, J.P., 2000. Endogenous retroviruses and the human germline. Current opinion in genetics & development 10 (6), 651–655.

Bodem, J., Schied, T., Gabriel, R., Rammling, M., Rethwilm, A., 2011. Foamy virus nuclear RNA export is distinct from that of other retroviruses. Journal of virology 85 (5), 2333–2341.

Bowers, K., Pitcher, C., Marsh, M., 1997. CD4: A co-receptor in the immune response and HIV infection. The International Journal of Biochemistry & Cell Biology 29 (6), 871–875.

Bukrinsky, M.I., Haggerty, S., Dempsey, M.P., Sharova, N., Adzhubel, A., Spitz, L., Lewis, P., Goldfarb, D., Emerman, M., Stevenson, M., 1993. A nuclear localization signal within HIV-1 matrix protein that governs infection of non-dividing cells. Nature 365 (6447), 666–669.

Büscher, K., Trefzer, U., Hofmann, M., Sterry, W., Kurth, R., Denner, J., 2005. Expression of human endogenous retrovirus K in melanomas and melanoma cell lines. Cancer research 65 (10), 4172–4180.

Carey, D.J., 1997. Syndecans: multifunctional cell-surface co-receptors. Biochemical Journal 327 (Pt 1), 1–16.

Cereseto, A., Mulloy, J.C., Franchini, G., 1996. Insights on the pathogenicity of human T-lymphotropic/leukemia virus types I and II. Journal of acquired immune deficiency syndromes and human retrovirology : official publication of the International Retrovirology Association 13 Suppl 1, S69-75.

Checkley, M.A., Luttge, B.G., Freed, E.O., 2011. HIV-1 envelope glycoprotein biosynthesis, trafficking, and incorporation. Journal of molecular biology 410 (4), 582–608.

Chen, J.C.-R., Zhang, J.P., Stephens, R.S., 1996. Structural Requirements of Heparin Binding to Chlamydia trachomatis. The Journal of biological chemistry 271 (19), 11134–11140.

Chiang, N.-Y., Chang, G.-W., Huang, Y.-S., Peng, Y.-M., Hsiao, C.-C., Kuo, M.-L., Lin, H.-H., 2016. Heparin interacts with the adhesion GPCR GPR56, reduces receptor shedding, and promotes cell adhesion and motility. Journal of cell science 129 (11), 2156–2169.

Choo, Q.L., Kuo, G., Weiner, A.J., Overby, L.R., Bradley, D.W., Houghton, M., 1989. Isolation of a cDNA clone derived from a blood-borne non-A, non-B viral hepatitis genome. Science (New York, N.Y.) 244 (4902), 359–362.

Clavel F., Guyader M., Guétard D., Sallé M., Montagnier L., Alizon M., 1986. Molecular cloning and polymorphism of the human immune deficiency virus type 2. Nature (324 (6098)), 691–695.

Clercq, E. de, 2007. The design of drugs for HIV and HCV. Nature reviews. Drug discovery 6 (12), 1001–1018.

Coffin JM., Hughes HS., Varmus HE., 1997. Book: Retroviruses. Cold Spring Harbor.

Coiras, M., López-Huertas, M.R., Sánchez del Cojo, M., Mateos, E., Alcamí, J., 2010. Dual role of host cell factors in HIV-1 replication: Restriction and enhancement of the viral cycle. AIDS reviews 12 (2), 103–112.

Compton, T., Nowlin, D.M., Cooper, N.R., 1993. Initiation of human cytomegalovirus infection requires initial interaction with cell surface heparan sulfate. Virology 193 (2), 834–841.

Connell, B.J., Lortat-Jacob, H., 2013. Human Immunodeficiency Virus and Heparan Sulfate: From Attachment to Entry Inhibition. Frontiers in Immunology 4.

Cooper, A., Tal, G., Lider, O., Shaul, Y., 2005. Cytokine induction by the hepatitis B virus capsid in macrophages is facilitated by membrane heparan sulfate and involves TLR2. Journal of immunology (Baltimore, Md. : 1950) 175 (5), 3165–3176.

Crawford LV., Cawford EM., 1961. The properties of Rous sarcoma virus purified by density gradient centrifugation. Virology (13), 227–232.

Cullen, B.R., 2002. Using retroviruses to study the nuclear export of mRNA. Results and problems in cell differentiation 35, 151–168.

David G, Lories V, Decock B, Marynen P, Cassiman JJ, Van den Berghe H., 1990. Molecular cloning of a phosphatidylinositol-anchored membrane heparan sulfate proteoglycan from human lung fibroblasts. The Journal of Cell Biology 111 (6), 3165–3176.

Deng, H., Liu, R., Ellmeier, W., Choe, S., Unutmaz, D., Burkhart, M., Di Marzio, P., Marmon, S., Sutton, R.E., Hill, C.M., Davis, C.B., Peiper, S.C., Schall, T.J., Littman, D.R., Landau, N.R., 1996. Identification of a major co-receptor for primary isolates of HIV-1. Nature 381 (6584), 661–666.

eenzyme. HIV Research Tools: http://www.eenzyme.com/HIVResearchTools-2.aspx.

Ellerman V., Bang O., 1908. Experimentelle Leukämie bei Hühnern. Zentralbl. Bakteriol. Parasitenkd. Infectionskr. Hyg. Abt. I. (46), 595–609.

Esko, J.D., 1991. Genetic analysis of proteoglycan structure, function and metabolism. Current opinion in cell biology 3 (5), 805–816.

Feng, Y., Broder, C.C., Kennedy, P.E., Berger, E.A., 1996. HIV-1 entry cofactor: Functional cDNA cloning of a seven-transmembrane, G protein-coupled receptor. Science (New York, N.Y.) 272 (5263), 872–877.

Fiebig, U., Hartmann, M.G., Bannert, N., Kurth, R., Denner, J., 2006. Transspecies transmission of the endogenous koala retrovirus. Journal of virology 80 (11), 5651–5654.

Freed, E.O., 2001. HIV-1 replication. Somatic cell and molecular genetics 26 (1-6), 13–33.

Funderburgh, J.L., 2000. Keratan sulfate: structure, biosynthesis, and function. Glycobiology 10 (10), 951–958.

Gallo RC., 2005. The discovery of the first human retrovirus: HTLV-1 and HTLV-2. Retrovirology (2), 17.

Ganser-Pornillos, B.K., Yeager, M., Sundquist, W.I., 2008. The structural biology of HIV assembly. Current opinion in structural biology 18 (2), 203–217.

George, M., Schwecke, T., Beimforde, N., Hohn, O., Chudak, C., Zimmermann, A., Kurth, R., Naumann, D., Bannert, N., 2011. Identification of the protease cleavage sites in a reconstituted Gag polyprotein of an HERV-K(HML-2) element. Retrovirology 8, 30.

Gifford, R., Tristem, M., 2003. The evolution, distribution and diversity of endogenous retroviruses. Virus genes 26 (3), 291–315.

Gifford RJ, 2006. Evolution at the host-retrovirus interface. Bioassays (28 (12)), 1153–1156.

Giroglou, T., Florin, L., Schäfer, F., Streeck, R.E., Sapp, M., 2001. Human Papillomavirus Infection Requires Cell Surface Heparan Sulfate. Journal of virology 75 (3), 1565–1570.

Götzinger, N., Sauter, M., Roemer, K., Mueller-Lantzsch, N., 1996. Regulation of human endogenous retrovirus-K Gag expression in teratocarcinoma cell lines and human tumours. The Journal of general virology 77 (Pt 12), 2983–2990.

Hallak, L.K., Collins, P.L., Knudson, W., Peeples, M.E., 2000. Iduronic acid-containing glycosaminoglycans on target cells are required for efficient respiratory syncytial virus infection. Virology 271 (2), 264–275.

Hanke, K., Hohn, O., Liedgens, L., Fiddeke, K., Wamara, J., Kurth, R., Bannert, N., 2013. Staufen-1 interacts with the human endogenous retrovirus family HERV-K(HML-2) rec and gag proteins and increases virion production. Journal of virology 87 (20), 11019–11030.

Herniou, E., Martin, J., Miller, K., Cook, J., Wilkinson, M., Tristem, M., 1998. Retroviral diversity and distribution in vertebrates. Journal of virology 72 (7), 5955–5966.

Hohn, O., Hanke, K., Bannert, N., 2013. HERV-K(HML-2), the Best Preserved Family of HERVs: Endogenization, Expression, and Implications in Health and Disease. Frontiers in oncology 3, 246.

Hohn, O., Mostafa, S., Norley, S., Bannert, N., 2016. Development of an antigen-capture ELISA for the detection of the p27-CA protein of HERV-K(HML-2). Journal of virological methods 234, 186–192.

Isaacs, R.D., 1994. Borrelia burgdorferi bind to epithelial cell proteoglycans. Journal of Clinical Investigation 93 (2), 809–819.

Jackson, T., Ellard, F.M., Ghazaleh, R.A., Brookes, S.M., Blakemore, W.E., Corteyn, A.H., Stuart, D.I., Newman, J.W., King, A.M., 1996. Efficient infection of cells in culture by type O foot-and-mouth disease virus requires binding to cell surface heparan sulfate. Journal of virology 70 (8), 5282–5287.

Jmarchn, 2017. The HIV replication cycle. wikimedia (https://commons.wikimedia.org/wiki/File:HIV-replication-cycle-en.svg).

Ju G., Skalka AM., 1980. Nucleotide sequence analysis of the long terminal repeat (LTR) of avian retroviruses: structural similarities with transposable elements. Cell (22 (2 Pt 2)), 379–386.

Kämmerer, U., Germeyer, A., Stengel, S., Kapp, M., Denner, J., 2011. Human endogenous retrovirus K (HERV-K) is expressed in villous and extravillous cytotrophoblast cells of the human placenta. Journal of reproductive immunology 91 (1-2), 1–8.

Katzourakis, A., Tristem, M., Pybus, O.G., Gifford, R.J., 2007. Discovery and analysis of the first endogenous lentivirus. Proceedings of the National Academy of Sciences of the United States of America 104 (15), 6261–6265.

Kim, C.W., Goldberger, O.A., Gallo, R.L., Bernfield, M., 1994. Members of the syndecan family of heparan sulfate proteoglycans are expressed in distinct cell-, tissue-, and development-specific patterns. Molecular Biology of the Cell 5 (7), 797–805.

Kjellén, L., Lindahl, U., 1991. Proteoglycans: structures and interactions. Annual review of biochemistry 60, 443–475.

Kraus, B., Boller, K., Reuter, A., Schnierle, B.S., 2011. Characterization of the human endogenous retrovirus K Gag protein: Identification of protease cleavage sites. Retrovirology 8, 21.

Krone, B., Grange, J.M., 2010. Melanoma, Darwinian medicine and the inner world. Journal of cancer research and clinical oncology 136 (12), 1787–1794.

Kurth R., Bannert N., 2010. Retroviruses: Molecular Biology, Genomics and Pathogenesis. Caister Academic Press.

LAEMMLI, U.K., 1970. Cleavage of Structural Proteins during the Assembly of the Head of Bacteriophage T4. Nature 227 (5259), 680–685.

Lander, E.S., Linton, L.M., Birren, B., Nusbaum, C., Zody, M.C., Baldwin, J., Devon, K., Dewar, K., Doyle, M., FitzHugh, W., Funke, R., Gage, D., Harris, K., Heaford, A., Howland, J., Kann, L., Lehoczky, J., LeVine, R., McEwan, P., McKernan, K., Meldrim, J., Mesirov, J.P., Miranda, C., Morris, W., Naylor, J., Raymond, C., Rosetti, M., Santos, R., Sheridan, A., Sougnez, C., Stange-Thomann, Y., Stojanovic, N., Subramanian, A., Wyman, D., Rogers, J., Sulston, J., Ainscough, R., Beck, S., Bentley, D., Burton, J., Clee, C., Carter, N., Coulson, A., Deadman, R., Deloukas, P., Dunham, A., Dunham, I., Durbin, R., French, L., Grafham, D., Gregory, S., Hubbard, T., Humphray, S., Hunt, A., Jones, M., Lloyd, C., McMurray, A., Matthews, L., Mercer, S., Milne, S., Mullikin, J.C., Mungall, A., Plumb, R., Ross, M., Shownkeen, R., Sims, S., Waterston, R.H., Wilson, R.K., Hillier, L.W., McPherson, J.D., Marra, M.A., Mardis, E.R., Fulton, L.A., Chinwalla, A.T., Pepin, K.H., Gish, W.R., Chissoe, S.L., Wendl, M.C., Delehaunty, K.D., Miner, T.L., Delehaunty, A., Kramer, J.B., Cook, L.L., Fulton, R.S., Johnson, D.L., Minx, P.J., Clifton, S.W., Hawkins, T., Branscomb, E., Predki, P., Richardson, P., Wenning, S., Slezak, T., Doggett, N., Cheng, J.F., Olsen, A., Lucas, S., Elkin, C., Uberbacher, E., Frazier, M., Gibbs, R.A., Muzny, D.M., Scherer, S.E., Bouck, J.B., Sodergren, E.J., Worley, K.C., Rives, C.M., Gorrell, J.H., Metzker, M.L., Naylor, S.L., Kucherlapati, R.S., Nelson, D.L., Weinstock, G.M., Sakaki, Y., Fujiyama, A.,

Hattori, M., Yada, T., Toyoda, A., Itoh, T., Kawagoe, C., Watanabe, H., Totoki, Y., Taylor, T., Weissenbach, J., Heilig, R., Saurin, W., Artiguenave, F., Brottier, P., Bruls, T., Pelletier, E., Robert, C., Wincker, P., Smith, D.R., Doucette-Stamm, L., Rubenfield, M., Weinstock, K., Lee, H.M., Dubois, J., Rosenthal, A., Platzer, M., Nyakatura, G., Taudien, S., Rump, A., Yang, H., Yu, J., Wang, J., Huang, G., Gu, J., Hood, L., Rowen, L., Madan, A., Qin, S., Davis, R.W., Federspiel, N.A., Abola, A.P., Proctor, M.J., Myers, R.M., Schmutz, J., Dickson, M., Grimwood, J., Cox, D.R., Olson, M.V., Kaul, R., Shimizu, N., Kawasaki, K., Minoshima, S., Evans, G.A., Athanasiou, M., Schultz, R., Roe, B.A., Chen, F., Pan, H., Ramser, J., Lehrach, H., Reinhardt, R., McCombie, W.R., La Bastide, M. de, Dedhia, N., Blöcker, H., Hornischer, K., Nordsiek, G., Agarwala, R., Aravind, L., Bailey, J.A., Bateman, A., Batzoglou, S., Birney, E., Bork, P., Brown, D.G., Burge, C.B., Cerutti, L., Chen, H.C., Church, D., Clamp, M., Copley, R.R., Doerks, T., Eddy, S.R., Eichler, E.E., Furey, T.S., Galagan, J., Gilbert, J.G., Harmon, C., Hayashizaki, Y., Haussler, D., Hermjakob, H., Hokamp, K., Jang, W., Johnson, L.S., Jones, T.A., Kasif, S., Kaspryzk, A., Kennedy, S., Kent, W.J., Kitts, P., Koonin, E.V., Korf, I., Kulp, D., Lancet, D., Lowe, T.M., McLysaght, A., Mikkelsen, T., Moran, J.V., Mulder, N., Pollara, V.J., Ponting, C.P., Schuler, G., Schultz, J., Slater, G., Smit, A.F., Stupka, E., Szustakowki, J., Thierry-Mieg, D., Thierry-Mieg, J., Wagner, L., Wallis, J., Wheeler, R., Williams, A., Wolf, Y.I., Wolfe, K.H., Yang, S.P., Yeh, R.F., Collins, F., Guyer, M.S., Peterson, J., Felsenfeld, A., Wetterstrand, K.A., Patrinos, A., Morgan, M.J., Jong, P. de, Catanese, J.J., Osoegawa, K., Shizuya, H., Choi, S., Chen, Y.J., 2001. Initial sequencing and analysis of the human genome. Nature 409 (6822), 860–921.

Leboyer, M., Tamouza, R., Charron, D., Faucard, R., Perron, H., 2013. Human endogenous retrovirus type W (HERV-W) in schizophrenia: A new avenue of research at the gene-environment interface. The world journal of biological psychiatry : the official journal of the World Federation of Societies of Biological Psychiatry 14 (2), 80–90.

Li, J.-P., Vlodavsky, I., 2009. Heparin, heparan sulfate and heparanase in inflammatory reactions. Thrombosis and haemostasis 102 (5), 823–828.

Liang, O.D., Flock, J.I., Wadström, T., 1995. Isolation and characterisation of a vitronectin-binding surface protein from Staphylococcus aureus. Biochimica et biophysica acta 1250 (1), 110–116.

Lindahl, U., 1990. Biosynthesis of heparin. Biochemical Society transactions 18 (5), 803–805.

Linhardt, R.J., Turnbull, J.E., Wang, H.M., Loganathan, D., Gallagher, J.T., 1990. Examination of the substrate specificity of heparin and heparan sulfate lyases. Biochemistry 29 (10), 2611–2617.

Liu, J., Thorp, S.C., 2002. Cell surface heparan sulfate and its roles in assisting viral infections. Medicinal research reviews 22 (1), 1–25.

Love DC, 1993. A heparin-binding activity on Leishmania amastigotes which mediates adhesion to cellular proteoglycans. The Journal of Cell Biology 123 (3), 759–766.

Luo, R., Jin, Z., Deng, Y., Strokes, N., Piao, X., 2012. Disease-associated mutations prevent GPR56-collagen III interaction. PloS one 7 (1), e29818.

Malassiné, A., Blaise, S., Handschuh, K., Lalucque, H., Dupressoir, A., Evain-Brion, D., Heidmann, T., 2007. Expression of the fusogenic HERV-FRD Env glycoprotein (syncytin 2) in human placenta is restricted to villous cytotrophoblastic cells. Placenta 28 (2-3), 185–191.

Maldonado, J.O., Martin, J.L., Mueller, J.D., Zhang, W., Mansky, L.M., 2014. New insights into retroviral Gag-Gag and Gag-membrane interactions. Frontiers in microbiology 5, 302.

Mi, S., Lee, X., Li, X., Veldman, G.M., Finnerty, H., Racie, L., LaVallie, E., Tang, X.Y., Edouard, P., Howes, S., Keith, J.C., McCoy, J.M., 2000. Syncytin is a captive retroviral envelope protein involved in human placental morphogenesis. Nature 403 (6771), 785–789.

Mikami, T., Kitagawa, H., 2013. Biosynthesis and function of chondroitin sulfate. Biochimica et biophysica acta 1830 (10), 4719–4733.

Modrow S., Falke D., Truyen U., Schaetzl H., 2009. Retroviren. Molekulare Virologie (3. Auflage), 409–459.

Nasimuzzaman, M., Persons, D.A., 2012. Cell Membrane–associated Heparan Sulfate Is a Receptor for Prototype Foamy Virus in Human, Monkey, and Rodent Cells. Molecular Therapy 20 (6), 1158–1166.

Nermut, M.V., Hockley, D.J., 1996. Comparative morphology and structural classification of retroviruses. Current topics in microbiology and immunology 214, 1–24.

Ono, A., 2009. HIV-1 Assembly at the Plasma Membrane: Gag Trafficking and Localization. Future virology 4 (3), 241–257.

Ortega-Barria, E., Pereira, M.E., 1991. A novel T. cruzi heparin-binding protein promotes fibroblast adhesion and penetration of engineered bacteria and trypanosomes into mammalian cells. Cell 67 (2), 411–421.

Özel, M., Pauli, G., Gelderblom, H.R., 1988. The organization of the envelope projections on the surface of HIV. Archives of Virology 100 (3-4), 255–266.

Perrimon, N., Bernfield, M., 2000. Specificities of heparan sulphate proteoglycans in developmental processes. Nature 404 (6779), 725–728.

Plochmann, K., Horn, A., Gschmack, E., Armbruster, N., Krieg, J., Wiktorowicz, T., Weber, C., Stirnnagel, K., Lindemann, D., Rethwilm, A., Scheller, C., 2012. Heparan sulfate is an attachment factor for foamy virus entry. Journal of virology 86 (18), 10028–10035.

Poiesz BJ., Ruscetti FW., Gazdar AF., Bunn PA., Minna JD., Gallo RC., 1980. Detection and isolation of type C retrovirus particles from fresh and cultured lymphocytes of a patient with cutaneous T-cell lymphoma. Proc Natl Acad Sci USA. (77), 7415–7419.

Pötgens, A.J.G., Drewlo, S., Kokozidou, M., Kaufmann, P., 2004. Syncytin: The major regulator of trophoblast fusion? Recent developments and hypotheses on its action. Human reproduction update 10 (6), 487–496.

Quigley, J.P., Rifkin, D.B., Reich, E., 1971. Phospholipid composition of Rous sarcoma virus, host cell membranes and other enveloped RNA viruses. Virology 46 (1), 106–116.

Reed, R., 2003. Coupling transcription, splicing and mRNA export. Current opinion in cell biology 15 (3), 326–331.

Reuss, F.U., Schaller, H.C., 1991. cDNA sequence and genomic characterization of intracisternal A-particle-related retroviral elements containing an envelope gene. Journal of virology 65 (11), 5702–5709.

Robinson-McCarthy, L.R., McCarthy, K.R., Raaben, M., Piccinotti, S., Nieuwenhuis, J., Stubbs, S.H., Bakkers, M.J.G., Whelan, S.P.J., 2018. Reconstruction of the cell entry pathway of an extinct virus. PLoS pathogens 14 (8), e1007123.

Roderiquez, G., Oravecz, T., Yanagishita, M., Bou-Habib, D.C., Mostowski, H., Norcross, M.A., 1995. Mediation of human immunodeficiency virus type 1 binding by interaction of cell surface heparan sulfate proteoglycans with the V3 region of envelope gp120-gp41. Journal of virology 69 (4), 2233–2239.

Rostand, K.S., Esko, J.D., 1997. Microbial adherence to and invasion through proteoglycans. Infection and Immunity 65 (1), 1–8.

Rous P., 1911. A sarcoma of the fowl transmissible by an agent separable from the tumor cells. J. Exp. Med. (13), 397–411.

Shi, Q., Jiang, J., Luo, G., 2013. Syndecan-1 serves as the major receptor for attachment of hepatitis C virus to the surfaces of hepatocytes. Journal of virology 87 (12), 6866–6875.

Shieh, M.T., 1992. Cell surface receptors for herpes simplex virus are heparan sulfate proteoglycans. The Journal of Cell Biology 116 (5), 1273–1281.

Shukla, D., Liu, J., Blaiklock, P., Shworak, N.W., Bai, X., Esko, J.D., Cohen, G.H., Eisenberg, R.J., Rosenberg, R.D., Spear, P.G., 1999. A novel role for 3-O-sulfated heparan sulfate in herpes simplex virus 1 entry. Cell 99 (1), 13–22.

Shukla, D., Spear, P.G., 2001. Herpesviruses and heparan sulfate: an intimate relationship in aid of viral entry. Journal of Clinical Investigation 108 (4), 503–510.

Smit, A.F., 1999. Interspersed repeats and other mementos of transposable elements in mammalian genomes. Current opinion in genetics & development 9 (6), 657–663.

Sonawane, N.D., Szoka, F.C., Verkman, A.S., 2003. Chloride accumulation and swelling in endosomes enhances DNA transfer by polyamine-DNA polyplexes. The Journal of biological chemistry 278 (45), 44826–44831.

Summerford, C., Samulski, R.J., 1998. Membrane-Associated Heparan Sulfate Proteoglycan Is a Receptor for Adeno-Associated Virus Type 2 Virions. Journal of virology 72 (2), 1438–1445.

Swanstrom, R., Wills, J.W., 1997. Retroviruses: Synthesis, Assembly, and Processing of Viral Proteins, Cold Spring Harbor (NY).

Teissier, E., Penin, F., Pécheur, E.-I., 2010. Targeting cell entry of enveloped viruses as an antiviral strategy. Molecules (Basel, Switzerland) 16 (1), 221–250.

Temin HM, 1964. Nature of the provirus of Rous sarcoma. Nat Cancer Inst Monogr. (17), 557–570.

Temin HM, 1963. Separation of morphological conversion and virus production in Rous sarcoma virus infection. Cold Spring Harbor Symp Quant Biol. (27), 407–414.

Ting, C.N., Rosenberg, M.P., Snow, C.M., Samuelson, L.C., Meisler, M.H., 1992. Endogenous retroviral sequences are required for tissue-specific expression of a human salivary amylase gene. Genes & development 6 (8), 1457–1465.

Tritel, M., Resh, M.D., 2000. Kinetic analysis of human immunodeficiency virus type 1 assembly reveals the presence of sequential intermediates. Journal of virology 74 (13), 5845–5855.

Turnbull, J.E., Fernig, D.G., Ke, Y., Wilkinson, M.C., Gallagher, J.T., 1992. Identification of the basic fibroblast growth factor binding sequence in fibroblast heparan sulfate. The Journal of biological chemistry 267 (15), 10337–10341.

van Nie, R., Verstraeten, A.A., Moes, J. de, 1977. Genetic transmission of mammary tumour virus by gr mice. Int. J. Cancer 19 (3), 383–390.

Vogt VM, Simon MN, 1999. Mass Determination of Rous Sarcoma Virus Virions by Scanning Transmission. J Virol. (73 (8)), 7050–7055.

Wang-Johanning, F., Frost, A.R., Jian, B., Azerou, R., Lu, D.W., Chen, D.-T., Johanning, G.L., 2003. Detecting the expression of human endogenous retrovirus E envelope transcripts in human prostate adenocarcinoma. Cancer 98 (1), 187–197.

Weiss, R.A., 2006. The discovery of endogenous retroviruses. Retrovirology 3, 67.

Wodrich, H., Kräusslich, H.G., 2001. Nucleocytoplasmic RNA transport in retroviral replication. Results and problems in cell differentiation 34, 197–217.

WuDunn, D., Spear, P.G., 1989. Initial interaction of herpes simplex virus with cells is binding to heparan sulfate. Journal of virology 63 (1), 52–58.

Zhang, X., Shi, J., Ye, X., Ku, Z., Zhang, C., Liu, Q., Huang, Z., 2017. Coxsackievirus A16 utilizes cell surface heparan sulfate glycosaminoglycans as its attachment receptor. Emerging microbes & infections 6 (7), e65.

Zhou, H., Xu, M., Huang, Q., Gates, A.T., Zhang, X.D., Castle, J.C., Stec, E., Ferrer, M., Strulovici, B., Hazuda, D.J., Espeseth, A.S., 2008. Genome-scale RNAi screen for host factors required for HIV replication. Cell host & microbe 4 (5), 495–504.

Zhu, W., Li, J., Liang, G., 2011. How does cellular heparan sulfate function in viral pathogenicity? Biomedical and environmental sciences : BES 24 (1), 81–87.

Declaration related to §20 (1)

I, Philipp Geppert, confirm that this Master Thesis submitted for assessment is my own and expressed in my own words. I did not use any other sources or aid than those in the reference list.

Place and date	Philipp Geppert